bioRxiv preprint doi: https://doi.org/10.1101/607622; this version posted April 12, 2019. The copyright holder for this preprint (which was not certified by peer review) is the author/funder, who has granted bioRxiv a license to display the preprint in perpetuity. It is made available under aCC-BY 4.0 International license.

Evidence for the role of extrusomes in evading attack by the host immune system in a scuticociliate parasite

Iria Folgueira[1], Jesús Lamas[2], Ana Paula De Felipe[1], Rosa Ana Sueiro[1], José Manuel Leiro[1,*]

[1]*Departamento de Microbiología y Parasitología, Instituto de Investigación y Análisis Alimentarios, Campus Vida, Universidad de Santiago de Compostela, Spain*

[2]*Departamento de Biología Funcional, Instituto de Acuicultura, Campus Vida, Universidad de Santiago de Compostela, Spain*

SHORT TITLE: Defensive role of extrusomes in scuticociliate parasites

*Author for correspondence:
Laboratorio de Parasitología,
Instituto de Investigación y Análisis Alimentarios,
Universidad de Santiago de Compostela,
C/ Constantino Candeira s/n, Campus Vida,
15875, Santiago de Compostela, La Coruña, Spain.

bioRxiv preprint doi: https://doi.org/10.1101/607622; this version posted April 12, 2019. The copyright holder for this preprint (which was not certified by peer review) is the author/funder, who has granted bioRxiv a license to display the preprint in perpetuity. It is made available under aCC-BY 4.0 International license.

Abstract

Like other ciliates, the scuticociliate parasite of turbot, *Philasterides dicentrarchi*, produces only a feeding or growing stage called a trophont during its life cycle. Exposure of the trophonts to immune serum extracted from the host and containing specific antibodies that induce agglutination / immobilization leads to the production of a mucoid capsule from which the trophonts later emerge. We investigated how these capsules are generated, observing that the mechanism was associated with the process of exocytosis involved in the release of a matrix material from the extrusomes. The extruded material contains mucin-like glycoproteins that are deposited on the surface of the cell and whose expression increases with time of exposure to the turbot antibodies, at both protein expression and gene expression levels. Stimulation of the trophonts with host immune serum also causes an increase in discharge of the intracellular storage compartments of calcium necessary for the exocytosis processes in the extrusomes. The results obtained suggest that *P. dicentrarchi* uses the extrusion mechanism to generate a physical barrier protecting the ciliate from attack by soluble factors of the host immune system. Data on the proteins involved and the potential development of molecules that interfere with this exocytic process could contribute to the development of glycosylated recombinant vaccines and drugs to improve the prevention and control of scuticociliatosis in turbot.

Keywords: *Philasterides dicentrarchi*, turbot, exocytosis, extrusomes, trichocyst matrix proteins, mucin-like glycoproteins.

bioRxiv preprint doi: https://doi.org/10.1101/607622; this version posted April 12, 2019. The copyright holder for this preprint (which was not certified by peer review) is the author/funder, who has granted bioRxiv a license to display the preprint in perpetuity. It is made available under aCC-BY 4.0 International license.

Introduction

Exocytosis may be an important mechanism of communication between microbes. Indeed, some microorganisms can develop highly specialized exocytotic organelles via the extrusion of different materials with important roles in mechanisms enabling adaptation to different environmental conditions [1]. Several groups of protozoa possess different types of exocytotic extrusive organelles, known as extrusomes. These organelles are associated with the cell membrane and have different structures containing a material that is usually expelled or extruded from the cell and that participates in different functions [2]. In ciliates, most extrusomes belong to the trichocyst type, which are characteristically spindle shaped and can quickly download their protein content in the form of a projectile in response to mechanical or physical stimuli, and with a probable function in defence against predators [3]. Other common extrusomes in some groups of ciliates include the toxicysts and haptocysts, which contain toxic material or can extrude material capable of penetrating the prey; both have a possible predatory function for prey capture and food uptake [4,5]. The function of trichites-type extrusomes, rod-shaped organelles circumferentially arranged in plasma pockets [6], is not yet completely known. However, it is believed that they can act as defensive or offensive elements [7]. Mucocysts and cortical granules, a special type of mucocysts, secrete an amorphous mucilaginous protective material on the cell surface. In some species, this material may be involved in the formation of cysts or temporary capsules with a protective role and constituting a first line of defence against predators in the ciliate, regulating cell ionic concentration and anchoring cells to substrates [3, 8-10].

Philasterides dicentrarchi is an amphizoic scuticociliate, originally free-living, which under certain conditions can be transformed into an opportunistic histiophagous parasite in cultivated flat fish, causing a serious disease called scuticociliatosis and producing high mortality rates [11,12]. In order to produce the parasitic phase, the ciliate must develop various strategies of biochemical adaptation to its new habitat [13,14]. In addition, it must evade attack by the fish immune system, especially by lysis induced by soluble factors in the serum, such as complement. Activation of complement via the classical route (in conjunction with antibodies), together with activation of the coagulation system, causes destruction of the parasite [15-17]. Two types of extrusomes

bioRxiv preprint doi: https://doi.org/10.1101/607622; this version posted April 12, 2019. The copyright holder for this preprint (which was not certified by peer review) is the author/funder, who has granted bioRxiv a license to display the preprint in perpetuity. It is made available under aCC-BY 4.0 International license.

have been characterized in *P. dicentrarchi*: one fusiform, compatible with trichocysts, and the other spherical, compatible with mucocysts, and which release a thin layer of mucus on the cell surface [18,19]. In previous studies, we have observed that incubation (for 2h) of *P. dicentrarchi* trophonts with serum from turbot that had survived a natural outbreak of scuticociliatosis caused agglutination and immobilization of the ciliates and the appearance of numerous capsules from which the trophonts later emerged. We interpreted this phenomenon as a possible antigenic change and a mechanism of evasion of the humoral immune response [20].

In the present study, we aimed i) to elucidate the role of the extrusomes in capsule production induced by incubation of the trophonts of *P. dicentrarchi* with immune sera from vaccinated turbot that produce agglutinating and immobilizing antibodies, ii) to characterize the proteins of the trichocysts and mucocysts after extrusion, and iii) to demonstrate the role of the process of exocytosis as a ciliate defence mechanism against attack by the soluble factors of the host humoral immune system.

Materials and Methods

Parasites

Specimens of *P. dicentrarchi* (isolate I1) were collected under aseptic conditions from peritoneal fluid obtained from experimentally infected turbot (*Scophthalmus maximus)*, as previously described [21]. The ciliates were cultured at 21 °C in complete sterile L-15 medium, as previously described [20]. In order to maintain the virulence of the ciliates, fish were experimentally infected every 6 months by intraperitoneal (ip) injection of 200 µL of sterile physiological saline containing $5x10^5$ trophonts, and the ciliates were recovered from ascitic fluid and maintained in culture as described above.

Experimental animals

Turbot of approximately 50 g body weight were obtained from a local fish farm. The fish were held in 250-L tanks with aerated recirculating sea water maintained at 14 °C. They were subjected to a photoperiod of 12L:12D and fed daily with commercial

bioRxiv preprint doi: https://doi.org/10.1101/607622; this version posted April 12, 2019. The copyright holder for this preprint (which was not certified by peer review) is the author/funder, who has granted bioRxiv a license to display the preprint in perpetuity. It is made available under aCC-BY 4.0 International license.

pellets (Skretting, Burgos, Spain). The fish were acclimatized to laboratory conditions for 2 weeks before the start of the experiments.

Swiss ICR (CD-1) mice (eight to ten weeks old), supplied by Charles River Laboratories (USA), were bred and maintained in the Central Animal Facility of the University of Santiago de Compostela (Spain). The mice were reared following the criteria for the protection, control, care and welfare of animals and the legislative requirements relating to the use of animals for experimentation (EU Directive 86/609/EEC), the Declaration of Helsinki, and/or the Guide for the Care and Use of Laboratory Animals as adopted and promulgated by the US National Institutes of Health (NIH Publication No. 85–23, revised 1996). The Institutional Animal Care and Use Committee of the University of Santiago de Compostela approved all experimental protocols.

Microscopic analysis

Scanning electron microscopy (SEM)

Ciliates treated with turbot immune serum (see Immunization and serum collection), were collected by centrifugation at 1000 x g, were fixed with 2.5% (v/w) glutaraldehyde in a cold solution of 4% paraformaldehyde in 0.1 M potassium phosphate buffer (PB), pH 7.2 for 30 min. The samples were post-fixed for 30 minutes with 1% (wt/v) osmium tetroxide in PB. The samples were then washed three times with distilled water and dehydrated in a series of ethanol (50, 70, 90, 95, 100, 100% for 10 min each) and hexamethyldisilazane (HMDS, Sigma-Aldrich) (50 and 100% for 10 min each). Finally, the samples were mounted on aluminium stubs, sputter coated with a layer of iridium, by using a Q150T-S sputter coater (Quorum Technologies, UK), and viewed under a Zeiss Fesem ultra plus microscope (Zeiss, Germany) at 10 kV.

Transmission electron microscopy (TEM)

For TEM, we followed the technique described by [19]. Briefly, the cultured ciliates were collected by centrifugation at 1000 x g for 5 min. Cells were fixed in 2.5% (v/v) glutaraldehyde in 0.1 M cacodylate buffer at pH 7.2. They were then washed several times with 0.1 M cacodylate buffer and post-fixed in 1% (wt/v) OsO_4, pre-stained

bioRxiv preprint doi: https://doi.org/10.1101/607622; this version posted April 12, 2019. The copyright holder for this preprint (which was not certified by peer review) is the author/funder, who has granted bioRxiv a license to display the preprint in perpetuity. It is made available under aCC-BY 4.0 International license.

in saturated aqueous uranyl acetate, dehydrated through a graded acetone series and embedded in Spurr's resin. Semi-thin sections were then cut with an ultratome (Leica Ultracut UCT, Leica microsystems, Germany) and stained with 1% toluidine blue for examination under a light microscope. Ultrathin sections were stained in alcoholic uranyl acetate and lead citrate and viewed in a Jeol JEM-1011 transmission electron microscope (Jeol, Japan) at an accelerating voltage of 100 kV.

Histochemistry: Safranin-O Staining

For detection of mucin-type proteins, the cells were stained with Safranin-O. Ciliates were incubated without turbot immune serum or with the serum for different times. The ciliates were fixed in 10% buffered formalin (PBS; 0.01 M Na_2HPO_4, 0.0018 M KH_2PO_4, 0.0027 M KCl, 0.137 M NaCl, pH 7.0). The samples were then washed 2 times with distilled water and incubated for 5 min with an aqueous solution of 0.1% of Safranin-O. After exhaustive washing with water to eliminate excess dye, the preparation was air-dried and mounted using a permanent mounting medium (Entellan®, Merck).

Trichocyst associated proteins

The sequences of several mRNAs that encode proteins potentially related to the trichocysts of *Philasterides dicentrarchi* were obtained from a previous RNAseq study carried out to compare the transcriptome of several *P. dicentrarchi* strains, in collaboration with ZF-Screen (Holland). The assembled sequences were analyzed using Blastgo software 5.0 (Biobam, Spain), to identify homologous sequences, before functional annotation. Annotated sequences that encode proteins potentially related to the trichocysts of ciliates were selected using the BLASTx tool of the TGD Wiki (http://www.ciliate.org/blast/blast_link.cgi) where the *Tetrahymena thermophila* gene and protein sequences database is located. To confirm the nucleotide sequences that encode the proteins associated with the extrusomes obtained by RNAseq, their cDNAs were amplified by RT-PCR and sequenced by Sanger Sequencing (Eurofins Genomics, Germany). The selected proteins associated with the extrusomes were the *P.*

bioRxiv preprint doi: https://doi.org/10.1101/607622; this version posted April 12, 2019. The copyright holder for this preprint (which was not certified by peer review) is the author/funder, who has granted bioRxiv a license to display the preprint in perpetuity. It is made available under aCC-BY 4.0 International license.

dicentrarchi trichocyst matrix protein T2A (TMPT2A) (GenBank accession number MH412657.1) and the *P. dicentrarchi* trichocyst matrix protein T4-B (TMPT4B) (GenBank accession number MH412658.1).

Production of recombinant proteins in yeast cells

The complete nucleotide sequence that encoded TMPT2A was modified and optimized to produce the recombinant protein in the yeast *Klyuveromyces lactis*, by using the bioinformatics tool developed by Integrated DNA Technology (IDT) (https://eu.idtdna.com/CodonOpt). The gene was then synthethized by Invitro GeneArt Gene Synthesis (ThermoFisher Scientific). For expression of recombinant protein in yeast, the *K. Lactis* Protein Expression kit (New England Biolabs, UK) was used with the pKLAC2 vector, following the instructions provided by the manufacturer. Initially, the synthesized nucleotide sequence was cloned in the pSpark® II vector (Canvax, Spain), and the recombinant plasmid was subsequently amplified in competent *Escherichia coli* strain DH-5α. After extraction and purification of the plasmid from the bacteria, PCR was carried out using the following primers: FT2AKl 5' CGCCTCGAGAAAAGAatgcgtgtctgaccgcacta-3' / RT2AKl 5-' ATAAGAATGCGGCCGCTTAATGATGATGGTGATGGTGATGATGGTGATGatcggcacgctttacgtc ga-3'. The reverse primer includes 10 codons encoding histidine at the C-terminal end of the protein. The yeasts were then transformed with the cloned pKLAC2 plasmid and seeded in YCB agar medium plates containing 5 mM acetamide at 30°C for 3–4 days until colony formation. Several of the colonies were collected and inoculated in the YPGal medium at 30 ºC for 3-4 days with shaking at 250 rpm. When a suitable cell density was reached, the medium was centrifuged at 6000 xg for 10 min, and the supernatant was held at 4 ºC until use. The protein was purified by submitting the supernatant to immobilized metal affinity chromatography (IMAC) using prepacked columns with Ni-Sepharose (HisTrap™, GE Healthcare) in an ÄKTA Star protein purification system (GE Healthcare) following the manufacturer's instructions. Once eluted, the protein was fully dialysed against distilled water using dialysis tubing of pore size 3 kDa. Finally, the protein was lyophilized and stored at 4 º C until use.

bioRxiv preprint doi: https://doi.org/10.1101/607622; this version posted April 12, 2019. The copyright holder for this preprint (which was not certified by peer review) is the author/funder, who has granted bioRxiv a license to display the preprint in perpetuity. It is made available under aCC-BY 4.0 International license.

Sodium dodecyl sulphate polyacrylamide gel electrophoresis (SDS-PAGE)

SDS-PAGE analysis of the recombinant TMPT2A (rTMPT2A) was performed on linear 12.5% polyacrylamide minigels in a Mini-Protean® Tetra cell system (BioRad, USA), as described by [22]. The gels consisted of 4% stacking gel and a 12.5% linear separating gel. Samples were dissolved in 62 mM Tris-HCl buffer (pH 6.8) containing 2% SDS, 10% glycerol and 0.004% bromophenol blue and heated for 5 min in a boiling water bath. The gels were electrophoresed at a constant 200 V in Tris-glycine electrode buffer (25 mM Tris, 190 mM glycine; pH 8.3). The gels were then fixed in 12% trichloroacetic acid for 1h and stained with QC Colloidal Coomassie stain (BioRad). Molecular weights were estimated using a calibration curve (Log_{10} MW vs Rf) constructed with a prestained protein standard (NZY Colour Protein Marker II, Nzytech, Portugal).

Immunization and serum collection

Turbot were immunized by intraperitoneal injection (i.p.) on days 0 and 30 with 200 µl of an emulsion containing 10^6 ciliates/mL inactivated with 0.2% formalin and 50% adjuvant Montanide ISA 763A (Seppic, France) [23]. Blood samples, obtained by caudal vein puncture, were allowed to clot for 2 h at room temperature before being centrifuged at 2000 x*g*. The serum was collected and stored at -20ºC until use.

A group of five ICR (Swiss) CD-1 mice were immunized by i.p. injection with 200 µL per mouse of a 1:1 (v/v) mixture of Freund's complete adjuvant (Sigma-Aldrich) and a solution containing 250 µg of purified rTMPT2A. The same dose of purified protein was prepared in Freund's incomplete adjuvant and injected i.p. in mice 15 and 30 days after the first immunization. The mice were bled via retrobulbar venous plexus 15 days after the last immunization (Day 30) for initial checking of the antibody levels. If the antibody levels were satisfactory, the mice were decapitated and immediately bled. The blood was allowed to coagulate overnight at 4ºC, and the serum was then separated by centrifugation (2000 xg for 10 min), mixed 1:1 with glycerol and stored at -20ºC until use.

bioRxiv preprint doi: https://doi.org/10.1101/607622; this version posted April 12, 2019. The copyright holder for this preprint (which was not certified by peer review) is the author/funder, who has granted bioRxiv a license to display the preprint in perpetuity. It is made available under aCC-BY 4.0 International license.

Immunological assays

Immobilization/agglutination assay

Cultured ciliates were washed 3 times in incomplete L-15 medium. Aliquots of 200 ciliates were added to individual wells of 96 well microplates (Corning, USA), in a final volume of 50 μL in L5-medium. Before the assay, the serum was heat-inactivated at 56 ºC for 30 min. The immune serum was assayed in triplicate and added to the wells containing the ciliates at dilutions of 1/25, 1/50 and 1/100 in L-15 medium. The plates were incubated at room temperature and checked for immobilization/agglutination responses, after 15, 30 and 60 min, under an inverted microscope (Nikon Eclipse TE300 Nikon, Japan). All assays included a ciliate control in incomplete L-15 medium with no serum. The agglutination response was expressed as the percentage of agglutinated ciliates.

Immunofluorescence and confocal microscopy

For immunolocalization of mucin-like proteins, an immunofluorescence assay was performed as previously described [24}. Briefly, $5x10^6$ ciliates incubated for different times with the immune serum from turbot, were centrifuged at 1000 xg for 5 min, washed twice with PBS pH 7.0 and fixed for 15 min in a solution of 4% formaldehyde in PBS at room temperature. The ciliates were then washed twice with PBS, resuspended in a solution containing 0·3% Triton X-100 in PBS for 3 min, washed twice with PBS, and incubated with 1% BSA for 30 min. After this blocking step, the ciliates were washed in PBS and incubated at room temperature with agitation (750 rpm) for an hour with a 1:100 dilution in PBS of mice serum anti-rTMPT2A. After being washed 3 times with PBS, the ciliate samples were added to a 1:1000 dilution of fluorescein isothiocyanate (FITC) conjugated rabbit/ anti-mouse Ig (DAKO, Denmark) and incubated for 1h at room temperature, in darkness. After another three washes in PBS, the samples were mounted in PBS-glycerol (1:1) and visualized by confocal microscopy (Leica TCS-SP2, Leica Microsystems, Germany).

bioRxiv preprint doi: https://doi.org/10.1101/607622; this version posted April 12, 2019. The copyright holder for this preprint (which was not certified by peer review) is the author/funder, who has granted bioRxiv a license to display the preprint in perpetuity. It is made available under aCC-BY 4.0 International license.

Fluorescent enzyme-linked immunosorbent assay (FELISA)

For quantification of the expression of the TMPT2A by the trophonts incubated with turbot immune serum for 30 min and 6h, a FELISA was conducted as previously described [14]. Ciliate lysate (CL), prepared as previously described [20], was used as antigen in the assay. One μg of CL isolated from trophonts dissolved in 100 μL of carbonate-bicarbonate buffer pH 9.6, was added to wells of ELISA microplates (high binding, Greiner Bio-One, Germany) and incubated overnight at 4ºC. The wells were then washed three times with 50 mM Tris, 0.15 M NaCl, pH 7.4 buffer (TBS), blocked for 1 h with TBS containing 0.2% Tween 20, 5% non-fat dry milk, incubated for 30 min at 37ºC in a microplate shaker at 750 rpm with 1:100 dilution of anti-rTMPT2A in TBS, and washed five times with TBS containing 0.05% Tween 20. Bound anti-mouse antibodies were detected with FITC-conjugated rabbit anti-mouse (Dako, Denmark) diluted 1:500 in TBS, after incubation for 30 min with shaking. After five washes in TBS, 100 μL of TBS was added to each well, and the fluorescence was measured in a microplate fluorescence reader (Bio-Tek Instruments, USA), at an excitation wavelength of 490 nm, and emission wavelength of 525 nm (sensitivity, 70%). The results are expressed in arbitrary fluorescence units.

Reverse transcriptase-quantitative polymerase chain reaction (RT-qPCR)

Aliquots of 10^6 trophonts/mL of *P. dicentrarchi* were incubated for 10, 60 and 240 min with turbot immune serum diluted 1:50 in incomplete L-15 medium. In some experiments, ciliates were incubated for 240 min with 500 μM of dibucaine hydrochloride (Sigma-Aldrich). Total RNA was isolated from the trophonts by using the NucleoSpin RNA isolation kit (Macherey-Nagel) according to the manufacturer's instructions. After purification of the RNA, the quality, purity and concentration were measured in a NanoDrop ND-1000 Spectrophotometer (NanoDrop Technologies, USA). The reaction mixture (25 μL) used for cDNA synthesis contained 1·25 μM random hexamer primers (Promega), 250 μM of each deoxynucleoside triphosphate (dNTP), 10 mM dithiothreitol (DTT), 20 U of RNase inhibitor, 2·5 mM $MgCl_2$, 200 U of Moloney murine leukemia virus reverse transcriptase (MMLV; Promega) in 30 mM Tris and 20 mM KCl (pH 8·3) and 2 μg of sample RNA. PCR (for cDNA amplification) was performed

bioRxiv preprint doi: https://doi.org/10.1101/607622; this version posted April 12, 2019. The copyright holder for this preprint (which was not certified by peer review) is the author/funder, who has granted bioRxiv a license to display the preprint in perpetuity. It is made available under aCC-BY 4.0 International license.

317 with gene-specific primers forward/reverse pair for the TMPT2A gene
318 (FTMPT2/RTMPT2) 5'- ATTTGCTTGCGTTCTCGTCT-3' / 5'- TCATCTTCGTCTTGGGCTCT-3';
319 TMPT4B gene (FTMPT4/ RTMPT4) 5'- CCACGAGAGATGGGTAGAGG-3' / 5'-
320 AATTCAATCTGGTGGCCAAT-3'. In parallel, a qPCR was performed with *P. dicentrarchi*
321 elongation factor 1-alpha gene (EF-1α) (GenBank accession KF952262) as a reference
322 gene, by including the forward/reverse primer pair (FEF1A/REF1A) 5'-
323 TCGCTCCTTCTTGCATCGTT-3'/ 5'- TCTGGCTGGGTCGTTTTTGT-3'). The Primer 3Plus
324 program was used, with default parameters, to design and optimize the primer sets.
325 Quantitative PCR mixtures (10 µL) contained 5 µL Kapa SYBR FAST qPCR Master Mix (2X)
326 (Sigma-Aldrich), 300 nM of the primer pair, 1 µL of cDNA and RNase-DNase-free water.
327 Quantitative PCR was developed at 95 °C for 5 min, followed by 40 cycles at 95 °C for 10
328 s and 60 °C for 30 s, ending with melting-curve analysis at 95 °C for 15 s, 55 °C for 15 s
329 and 95 °C for 15 s. qPCRs were performed in an Eco RT-PCR system (Illumina). Relative
330 quantification of gene expression was determined by the $2^{-\Delta\Delta Ct}$ method [25] applied
331 with software conforming to minimum information for publication of RT-qPCR
332 experiments (MIQE) guidelines [26].
333

334 ## Intracellular Ca^{2+} release analysis

335 The release of intracellular Ca^{2+} after stimulation of ciliates with turbot immune
336 serum was analyzed using the No-Wash, Fluo-4NW calcium assay kit (Life Technologies).
337 The ciliates ($2x10^5$) were washed twice by centrifugation with Hanks' balanced salt
338 solution (HBSS without Ca^{2+}, Mg^{2+}, and phenol red) and resuspended in assay medium
339 (HBSS, 20 mM HEPES and 2.5 mM probenecid) to a final concentration of $1.25x10^6$
340 ciliates/mL. The ciliates were then incubated with 1:50 dilution of turbot immune serum
341 in 96-well microplates at 21ºC. The cell-permeable Ca^{2+} indicator probe, Fluo-4 NW, was
342 added following the manufacturer's instructions, and the fluorescence (Ex: 494 nm, Em:
343 516 nm) was measured in a fluorimeter (FLx800, BioTek, USA). Negative controls with
344 HBSS were included.
345

346 ## Bioinformatic and statistical analysis

347 The performance of the functional analysis of proteins was evaluated and
348 families predicting the domains and important sites were classified using InterPro

bioRxiv preprint doi: https://doi.org/10.1101/607622; this version posted April 12, 2019. The copyright holder for this preprint (which was not certified by peer review) is the author/funder, who has granted bioRxiv a license to display the preprint in perpetuity. It is made available under aCC-BY 4.0 International license.

software [27]. The transmembrane topology and location of signal peptide cleavage sites in amino acid sequences were predicted using Phobius [28], SignalP [29] and Signal-3L 2.0 [30] software. Protein sequence motifs were searched for using the MotiFinder tool of the Japanese network GenomeNet (accessible on-line at: https://www.genome.jp/tools/motif/MOTIF.html). Mucin type GalNAc O-glycosylation sites were predicted using the NetOGlyc 4.0 Server [31]. The physicochemical parameters for a given protein were predicted using the ProtParam tool [32]. Protein modelling was conducted using the SWISS-MODEL server [33]. The cysteine and histidine metal binding sites of the sequenced protein were predicted using METALDETECTOR v2.0 [34]. The amino acid sequences of the TMPT2A and TMPT4B genes were aligned using Clustal Omega [35]. The evolutionary history was inferred using the Maximum Likelihood method based on the JTT matrix-based model [36]. Finally, evolutionary analyses were conducted in Mega7 [37].

The results are expressed as means ± standard error of the means (SEM). The data were examined by one-way analysis of variance (ANOVA) followed by the Tukey-Kramer test for multiple comparisons, and differences were considered significant at α=0.05.

RESULTS

Morphological changes produced in ciliates incubated with immune serum from the host

Immunization of turbot with a crude extract of ciliates-CL- generated sufficient levels of antibodies to induce immobilization/agglutination, with peak levels reached after one hour of incubation (Fig. 1). As already indicated, we used inactivated immune sera to prevent the lytic action of complement and to enable specific study of the processes produced exclusively by the action of the antibodies during agglutination/ immobilization of the trophonts.

The presence of agglutinating antibodies caused the agglutinated trophonts to produce a mucoid capsule, which became increasingly evident throughout the incubation period. After two hours of incubation, the ciliates began to emerge from the capsules, showing a normal morphology, and the number of free ciliates increased over

bioRxiv preprint doi: https://doi.org/10.1101/607622; this version posted April 12, 2019. The copyright holder for this preprint (which was not certified by peer review) is the author/funder, who has granted bioRxiv a license to display the preprint in perpetuity. It is made available under aCC-BY 4.0 International license.

time. The empty capsules showed the external morphology of the parasite. (Fig. 2). SEM-examination of the agglutination process clearly revealed the superficial changes that take place in the ciliate in the presence of the turbot immune serum over time (Fig. 3). The addition of the immune serum initially did not seem to affect the ciliates, whose ciliary morphology was apparently unchanged (time 0); however, during the incubation period the trophonts increased in diameter and a layer of gradually thicker amorphous material appeared on the surface. At the end of the process, microphotographs clearly show the presence of structures that maintain the external ciliary morphology but that are hollow. The free ciliates showed a normal ciliary structure (Fig. 3).

Molecular and biochemical characterization of the extrusome proteins

P. dicentrarchi has two types of extrusomes associated with the plasma membrane and located at the insertion sites between the alveolar sacs (Fig 4). Examination by electron microscopy revealed that the extrusomes have spherical morphology (Fig. 4A) or elongated morphology (Fig. 4B). Apart from the morphology, the characteristics of the material that these two types of extrusomes contain were also different. Thus, on the one hand, rounded extrusomes contained an electrolucent material (Fig. 4A), while elongated extrusomes contained greater amounts of electrodense material (Fig. 4B).

In order to identify possible proteins contained in the extrusomes, we used RNA sequencing technology. This enabled us to sequence the entire transcriptome of the ciliates and to locate the protein sequences that may be related to the extrusomes. After annotation of the genes that encode proteins of the parasite, using the BLASTx tool, we were able to detect proteins associated with extrusomes in other ciliates. Thus, homology analysis enabled us to detect two types of proteins related to extrusomes: 1) *P. dicentrarchi* trichocyst matrix protein T2-A (TMPT2A) (accession MH412657.1) encoded by an 1134 bp mRNA that generates a protein of 377 aa (Fig. 4C), of molecular weight 43502.79 daltons and a theoretical pI of 4.96 (Fig. 4E). This protein has a signal peptide between position 1 and 18 (Fig. 4C), with a cleavage site between position 18 and 19, corresponding to aa 15-18 with the signal peptide C-region, between aa 3-14 the signal peptide H-region is located and between the aa 1-2 the signal peptide N-region. The TMPT2A protein possesses 12 potential O-glycosylation sites in the aa 182,

bioRxiv preprint doi: https://doi.org/10.1101/607622; this version posted April 12, 2019. The copyright holder for this preprint (which was not certified by peer review) is the author/funder, who has granted bioRxiv a license to display the preprint in perpetuity. It is made available under aCC-BY 4.0 International license.

189, 195-196, 202, 210, 222-224, 317, 348 y 366 (Fig. 4C), and binds to metals in the cysteine at position 10. 2) *P. dicentrarchi* trichocyst matrix protein T4-B (TMPT4B) (accession MH412658.1) encoded by an 1113 bp mRNA and possesses 370 aa (Fig. 4D) of molecular weight of 41996.11 daltons and a theorical pI of 4.90 (Fig. 4F). The modeling of the structure of the proteins, using the Swiss-model, indicates that the oligomeric state of the two *P. dicentrarchi* trichocyst matrix proteins is monomeric. The protein has a signal peptide located between aa 1-16, according to the prediction by the Phobius program (Fig. 4D); however, the Signal-3L program predicts a signal peptide between aa 1 and 23. According to Phobius, the signal peptide C-region is located between aa 13 and 16, the signal peptide H-region between aa 4-12, and the signal peptide N-region between aa 1 and 3. This protein has 12 potential O-glycosylation sites in aas 21, 28, 54, 104, 111, 147, 218, 286, 291-292, 301 and 324 (Fig. 4D). BLAST analysis of the database including the *Tetrahymena thermophila* genome (TGD) indicated that this protein is related to a similar protein encoded by the GRL3 gene (Granule Lattice), which encodes the granule lattice protein and corresponds to an acidic, calcium-binding structural protein of dense core granules, contains coiled-coil region. This protein seems to possess a cysteine at position 16 (which may be a Ca^{2+}binding site), according to the prediction with METALDECTETOR v2.0 (cysteine and histidine metal binding sites predictor).

The TMPT2A and TMPT4B proteins displayed very low sequence identity (23%). The sequence identity was also very low in comparison with other ciliated proteins (e.g. *Paramecium, Ichtthyophthirius* and *Tetrahymena*) with maximum sequence identity scarcely exceeding 30%, for TMPT2A and TMPT4B (Figs. 5A, B; 6A, B). Phylogenetically, the TMPT2A protein is closer to *Paramecium* (Fig. 5C), while the TMPT4B protein is more phylogenetically spaced with the other ciliates analyzed (Fig. 6C).

When the ciliates incubated with turbot immune serum were stained with safranin-O dye, a progressive and time-dependent increase in the intensity of staining both in the cytoplasm and in the external material surrounding the ciliate was observed (Fig. 7).

bioRxiv preprint doi: https://doi.org/10.1101/607622; this version posted April 12, 2019. The copyright holder for this preprint (which was not certified by peer review) is the author/funder, who has granted bioRxiv a license to display the preprint in perpetuity. It is made available under aCC-BY 4.0 International license.

Expression and location of extrusome proteins after stimulation with immune serum from the host

In order to determine whether the proteins presumably associated with the trichocysts are involved in the formation of the capsules observed during the agglutination of the ciliates by the host immune serum, the recombinant protein was generated in the yeast *Kluyveromyces lactis*. For this purpose, we expressed the TMPT2A protein in the yeast (Fig. 8A), which was used to generate antisera in mice to enable us to perform experiments to study expression of this protein after incubation with the antiserum (Fig. 8B) and to determine the cytolocation (Fig. 8C).

First, the recombinant protein expressed by yeast has the biochemical characteristics (e.g. molecular size) predicted for the original sequence obtained from the ciliate, which indicates that this protein expression system is optimal for the heterologous expression of this type of eukaryotic proteins (Fig. 8A). On the other hand, the antibodies generated in mice against the rTMPT2A protein demonstrated that the material produced after incubation of ciliates with the turbot immune serum is related to this protein, as demonstrated by the FELISA assay, in which the absorbance levels of these antibodies increase during the period of incubation with the immune serum from turbot (Fig. 8B). By using immunofluorescence, an increase in fluorescence was observed in both the cytoplasm of the agglutinated ciliates and in the material associated with the outer surface throughout the incubation period (Fig. 8C).

Expression of the genes associated with extrusome proteins and their association with the discharge of intracellular Ca^{2+} after stimulation of the ciliates with host immune serum

We investigated expression of the genes encoding the trichocysts proteins TMPT2A, TMPT4B after incubation with the turbot immune serum for different times. Incubation of the ciliates with the turbot immune serum produced a significant increase in the mRNA levels of the genes encoding these proteins throughout the incubation period (Fig. 9A). Dibucaine, included as a positive control for the induction of extrusion, also had a stimulatory effect on the expression of both mRNA levels relative to the all

bioRxiv preprint doi: https://doi.org/10.1101/607622; this version posted April 12, 2019. The copyright holder for this preprint (which was not certified by peer review) is the author/funder, who has granted bioRxiv a license to display the preprint in perpetuity. It is made available under aCC-BY 4.0 International license.

473 trichocyst genes; however, the absolute mean values of increase were higher for the
474 TMPT2A gene than for the TMPT4B gene (Fig. 9A).
475 Finally, we analyzed the effect of the addition of turbot immune serum on the
476 intracellular Ca^{2+} discharge by using the Fluo-4NW probe. Incubation of the trophonts
477 with the turbot immune serum induced discharge of intracellular Ca^{2+} discharge, as
478 evidenced by the increase in fluorescence levels throughout the incubation time, while
479 the fluorescence increased only slightly over time in the ciliates not exposed to the
480 serum (Fig. 9B).
481
482 **Discussion**
483 In protists, extrusomes are specialized exocytotic and ejectable organelles which
484 can discharge their contents outside of the cell in response to external mechanical or
485 chemical stimuli and which can have offensive or defensive functions during predation
486 or in the acquisition of food [38]. In *P. dicentrarchi*, two types of extrusomes have been
487 described: a fusiform type (fibrous trichocysts) located in the cortex, perpendicular to
488 the plasma membrane, and a spherical type (mucocysts) with an irregular distribution
489 [18,19]. The mucocysts, which have an amorphous content, merge with the plasma
490 membrane and release their contents to the exterior giving rise to a thin mucilaginous
491 layer over the cell surface [19]. Although in free-living ciliates the extrusomes can have
492 a protective or defensive response to environmental changes, in ciliated parasites such
493 as *P. dicentrarchi*, the extrusomes may play a role in providing protection from attack by
494 the host immune system. The existence of the production of capsules by the trophonts
495 of *P. dicentrarchi* was initially obtained in studies of ciliate agglutination caused by
496 different immune sera from turbot and rabbit [20]. In those studies, it was observed that
497 when ciliates were incubated with the immune sera (for 2h), abundant transparent
498 capsule-like structures appeared. The precise surface topography of the ciliate, including
499 the somatic cilia could be seen and ciliates were also observed moving within the
500 capsules [20]. At that time, it was interpreted that their capsules probably made up of
501 immunocomplexes between these antigens and the agglutinating antibodies [20]. In the
502 present study, we sequentially monitored the agglutination of the trophonts by
503 inactivated immune turbot serum in order to investigate the capsule formation. The
504 phenomenon of capsule formation has already been described in the ciliates; e.g.

bioRxiv preprint doi: https://doi.org/10.1101/607622; this version posted April 12, 2019. The copyright holder for this preprint (which was not certified by peer review) is the author/funder, who has granted bioRxiv a license to display the preprint in perpetuity. It is made available under aCC-BY 4.0 International license.

505 *Tetrahymena* forms capsules when exocytosis of mature mucocysts is induced by the
506 secretagogue Alcian Blue 8GS [39-41]. In the environment, the ciliate mucocysts secrete
507 an amorphous material to protect the cell from osmotic shock or from predator attacks
508 [43].

509 The appearance of capsules during agglutination of the *P. dicentrarchi* trophonts
510 with immune serum suggests that the host antibodies induce the mucocysts to extrude
511 their mucilaginous content. This material is deposited on the surface of the ciliate
512 forming a protective layer, which eventually became a rigid capsule with an external
513 topology identical to that of the ciliate and which protects it from agglutination. This
514 process was clearly observed in this study by both optical microscopy and SEM.

515 In ciliates such as *Paramecium*, trichocysts are characterized by a highly
516 constrained shape that reflects the crystalline organization of the proteins that they
517 contain and that are derived from the process of a broad family of precursor proteins
518 (coded by a family of some 100 coexpressed genes) that allow correct processing of the
519 crystalline core assembly necessary for functioning of the trichocyst [44,45]. The
520 trichocyst matrix proteins in *Paramecium* are of sizes ranging between 15-20 kDa, and
521 some are glycosylated; the isoelectric points are between 4.7 and 5.5 and the proteins
522 seem to be derived from the proteolytic processing of precursor proteins of size
523 between 40-45 kDa [46,47]. In our study, the TMPT2A and TMPT4B proteins were about
524 43 kDa in size and the isoelectric points were close to 5.0, i.e. they are compatible with
525 the precursor proteins described in *Paramecium.* In addition, the proteins from *P.*
526 *dicentrarchi* possess sequences with a very low similarity to each other, although with
527 very similar isoelectric points and sizes. This may indicate that the trichocyst matrix is
528 composed of complex interrelated proteins, or of the proteolytic processing during the
529 maturation of secretory proteins [46], or of post-translational modifications [48]. It has
530 also been observed in *Paramecium tetraurelia* that proteins released by exocytosis of
531 trichocysts are glycoproteins [49].

532 As previously mentioned, apart from the encysting stages of the ciliates, capsule
533 production is rare, but has been induced *in vitro* in several species [42]. The capsule has
534 been shown to consist of mucopolysaccharide material from mucocysts [50,51].
535 *Tetrahymena* has mucocyst-type extrusomes characterized by containing mucin-like
536 acidic proteins of sizes between 40 and 80 kDa and that can bind to Ca^{2+} [8]. O-

bioRxiv preprint doi: https://doi.org/10.1101/607622; this version posted April 12, 2019. The copyright holder for this preprint (which was not certified by peer review) is the author/funder, who has granted bioRxiv a license to display the preprint in perpetuity. It is made available under aCC-BY 4.0 International license.

537 glycosylation (or "mucin-type O-glycosylation") indicates that these proteins carry this
538 type of glycan to the side-arm hydroxyl groups of serine and threonine residues [52].
539 Safranin O staining has been used to detect glycosaminoglycans [53] and mucins [54].
540 All mucins are highly O-glycosylated, and the biosynthesis and degradation are perfectly
541 integrated for protection of the cell against external aggressions [55]. The present
542 findings clearly show that the presence of antibodies in the turbot immune serum acts
543 as a stimulus that leads to the production of mucin-like proteins, as shown by Safranin
544 staining. The stimulation also causes a significant increase in the expression of both the
545 matrix proteins and the expression of the genes that encode them. The immunological
546 assays revealed that the components of the capsule share epitopes with the matrix
547 glycoproteins of the extrusomes.

548 In ciliate secretion systems, Ca^{+2} is necessary for stimulus-secretion coupling
549 [56]. In *Paramecium* it has been shown that the exocytic release of the paracrystalline
550 secretor product derived from the trichocyte matrix depends on Ca^{2+}, and the secretory
551 signal probably involves an influx of calcium [57,58]. The role of calcium in exocytosis
552 has been demonstrated in *Paramecium* following the application of Ca^{+2} ionophores,
553 and direct microinjection of Ca^{+2} in the cells induces exocytosis of the trichocysts [59].
554 On the other hand, in *Tetrahymena*, the addition of the anaesthetic dibucaine induces
555 the synchronous secretion of mature mucocysts [60] via an increase in intracellular Ca^{+2}
556 [61] and the release of flocculent mucin [8]. In this study, we demonstrated that
557 stimulation of *P. dicentrarchi* trophonts with antibodies in turbot serum induces
558 discharge of intracellular Ca^{+2} and extrusion.

559 In conclusion, our findings indicate that *P. dicentrarchi* can overcome the
560 agglutination generated by the specific antibodies produced by the host by generating
561 capsules through the extrusome-mediated secretion of O-glycosylated matrix proteins
562 that possess mucin-like characteristics, and whose release is regulated through Ca^{+2}-
563 mediated signalling. The findings show that the ciliate uses exocytosis as a defence
564 mechanism that probably allows evasion of the host immune response. Likewise,
565 analysis of the extrusome matrix proteins in yeast by heterologous production
566 technology, which has the advantage of producing glycosylated proteins, will allow us
567 to develop recombinant proteins of potential use in vaccines for the immunoprophylaxis
568 of scuticociliatosis in turbot.

bioRxiv preprint doi: https://doi.org/10.1101/607622; this version posted April 12, 2019. The copyright holder for this preprint (which was not certified by peer review) is the author/funder, who has granted bioRxiv a license to display the preprint in perpetuity. It is made available under aCC-BY 4.0 International license.

Acknowledgements

This study was financially supported by grants from the Ministerio de Economía y Competitividad (Spain) and Fondo Europeo de Desarrollo Regional -FEDER- (European Union) (AGL2017-83577-R) and from the Xunta de Galicia (Spain) (ED431C2017/31) and also by the PARAFISHCONTROL project, which received funding from the European Union's Horizon 2020 research and innovation programme under grant agreement No. 634429. This publication reflects the views of the authors, and the European Commission cannot be held responsible for any use which may be made of the information contained herein

References

1. Rosati G, Modeo L (2003) Extrusomes in ciliates: diversification, distribution, and phylogenetic implications. J Eukaryiot Microbiol 50: 383-402.

2. Taylor WD, Sanders RW (2010) Protozoa. In: Ecology and Classification of North American Freshwater Invertebrates. Third Edition, (Thorp, JH & Covich AP, Eds.). Academic Press, pp: 49-90.

3. Haacke-Bell B, Hohenberger-Bregger R, Plattner H (1990) Trichocysts of *Paramecium*: secretory organelles in search of their function. Eur J Protistol 25: 289-305.

4. Benwitz G (1984) Die Entladung der Haptocysten von *Ephelota gemmipara* (Suctoria, Ciliata). Z Naturforsch C 39: 812-817.

5. Ricci N, Morelli A, Verni F (1996) The predation of *Litonotus* on *Euplotes*: a two-step cell-cell recognition process. Acta Protozool 35: 201-208.

bioRxiv preprint doi: https://doi.org/10.1101/607622; this version posted April 12, 2019. The copyright holder for this preprint (which was not certified by peer review) is the author/funder, who has granted bioRxiv a license to display the preprint in perpetuity. It is made available under aCC-BY 4.0 International license.

592 6. Krainer KH (1991) Contribution to the morphology, infraciliature and ecology of the
593 planktonic ciliates *Strombidium pelagicum* n. sp., *Pelagostromhidium mirabile*
594 (Penard, 1916) n. g. n. comb., and *Pelagostrombidium fullax* (Zacharias, 1876) n.
595 g., n. comb. (Ciliophora, Oligotrichida). Eur J Protistol 27: 60-70.

596 7. Modeo L, Petroni G, Bonaldi M, Rosati G (2001) Trichites of *Strombidium* (Ciliophora,
597 Oligotrichida) are extrusomes. J Eukaryot Microbiol 48: 95-101.

598 8. Sauer MK, Kelly RB (1995) Conjugation rescue of exocytosis mutants in *Tetrahymena*
599 *thermophila* indicates the presence of functional intermediates in the regulated
600 secretory pathway. J Eukaryot Microbiol 42: 173-183.

601 9. Miyake A, Buonanno F, Saltalamachia P, Masaki ME, Lio H (2003) Chemical defence
602 by means of extrusive cortical granules in the heterotrich ciliate *Climacostomun*
603 *virens*. Eur J Protistol 39: 25-36.

604 10. Fyde J, Kennaway G, Adams K, Warren A (2006) Ultrastructural events in the
605 predator-induced defence response of *Colpidium kleini* (Ciliophora:
606 Humenostomatia). Acta Protozool 45: 461-464.

607 11. Iglesias R, Paramá A, Alvarez MF, Leiro J, Fernández J, et al. (2001)
608 *Philasterides dicentrarchi* (Ciliophora, Scuticociliatida) as the causative agent of
609 scuticociliatosis in farmed turbot *Scophthalmus maximus* in Galicia (NW Spain).
610 Dis Aquat Organ 46: 47-55.

bioRxiv preprint doi: https://doi.org/10.1101/607622; this version posted April 12, 2019. The copyright holder for this preprint (which was not certified by peer review) is the author/funder, who has granted bioRxiv a license to display the preprint in perpetuity. It is made available under aCC-BY 4.0 International license.

611 12. De Felipe AP, Lamas J, Sueiro RA, Folgueira I, Leiro JM (2017) New data on flatfish
612 scuticociliatosis reveal that *Miamiensis avidus* and *Philasterides dicentrarchi* are
613 different species. Parasitology 29: 1-18.

614 13. Mallo N, Lamas J, Leiro JM (2013) Evidence of an alternative oxidase pathway for
615 mitochondrial respiration in the scuticociliate *Philasterides dicentrarchi*. Protist
616 164: 824-836.

617 14. Mallo N, Lamas J, de Felipe AP, Sueiro RA, Fontenla F, et al. (2016). Role of H(+)-
618 pyrophosphatase activity in the regulation of intracellular pH in a scuticociliate
619 parasite of turbot: Physiological effects. Exp Parasitol 169: 59-68.

620 15. Piazzon MC, Wiegertjes GF, Leiro J, Lamas J. (2011) Turbot resistance
621 to *Philasterides dicentrarchi* is more dependent on humoral than on cellular
622 immune responses. Fish Shellfish Immunol 30: 1339-1347.

623 16. Piazzon MC, Leiro J, Lamas J (2014) Reprint of "fish immunity to scuticociliate
624 parasites". Dev Comp Immunol 43: 280-289.

625 17. Blanco-Abad V, Noia M, Valle A, Fontenla F, Folgueira I, De Felipe AP, Pereiro P, et
626 al. (2018) The coagulation system helps control infection caused by the ciliate
627 parasite *Philasterides dicentrarchi* in the turbot *Scophthalmus maximus* (L.). Dev
628 Comp Immunol 87: 147-156.

629 18. Dragesco A, Dragesco J, Coste F, Gasc C, Romestand B, et al. (1995) *Philasterides*
630 *dicentrarchi*, n. sp. (Ciliophora, Scuticociliatida), a histophagous opportunistic

bioRxiv preprint doi: https://doi.org/10.1101/607622; this version posted April 12, 2019. The copyright holder for this preprint (which was not certified by peer review) is the author/funder, who has granted bioRxiv a license to display the preprint in perpetuity. It is made available under aCC-BY 4.0 International license.

631 parasite of *Dicentrarchus labrax* (Linnaeus, 1758) a reared marine fish. Eur J
632 Protistol 31: 327-340.

633 19. Paramá A, Arranz JA, Alvarez MF, Sanmartín ML, Leiro J (2006) Ultrastructure and
634 phylogeny of *Philasterides dicentrarchi* (Ciliophora, Scuticociliatia) from farmed
635 turbot in NW Spain. Parasitology 132: 555-564.

636 20. Iglesias R, Paramá A, Alvarez MF, Leiro J, Ubeira FM, et al. (2003) *Philasterides*
637 *dicentrarchi* (Ciliophora:Scuticociliatida) expresses surface immobilization
638 antigens that probably induce protective immune responses in turbot.
639 Parasitology 126: 125-134.

640 21. Paramá A, Iglesias R, Álvarez M F, Leiro J, Aja C, et al. (2003) *Philasterides dicentrarchi*
641 (Ciliophora, Scuticociliatida): experimental infection and possible routes of entry
642 in farmed turbot (*Scophthalmus maximus*). Aquaculture 217: 73–80.

643 22. Iglesias R, Leiro J, Ubeira FM, Santamarina MT, Sanmartín ML (1993)
644 *Anisakis simplex*: antigen recognition and antibody production in experimentally
645 infected mice. Parasite Immunol 15: 243-250.

646 23. Lamas J, Sanmartín ML, Paramá A, Castro R, Cabaleiro S, et al. (2008). Optimization
647 of an inactivated vaccine against a scuticociliate parasite of turbot: Effect of
648 antigen, formalin and adjuvant concentration on antibody response and
649 protection against the pathogen. Aquaculture 278: 22-26.

650 24. Livak KJ, Schmittgen TD (2001) Analysis of relative gene expression data using real-
651 time quantitative PCR and the 2-(delta delta C(T)) method. Methods 25: 402-408

bioRxiv preprint doi: https://doi.org/10.1101/607622; this version posted April 12, 2019. The copyright holder for this preprint (which was not certified by peer review) is the author/funder, who has granted bioRxiv a license to display the preprint in perpetuity. It is made available under aCC-BY 4.0 International license.

652 25. Bustin SA, Benes V, Garson JA, Hellemans J, Huggett J, et al. (2009) The MIQE
653 guidelines: minimum information for publication of quantitative real-time PCR
654 experiments. Clin Chem 55: 611-622.

655 26. Mallo N, Lamas J, Piazzon C, Leiro JM (2015) Presence of a plant-like proton
656 translocating pyrophosphatase in a scuticociliate parasite and its role as a
657 possible drug target. Parasitology 142: 449–462.

658 27. Mitchell AL, Attwood TK, Babbitt PC, Blum M, Bork P, et al. (2019) InterPro in 2019:
659 improving coverage, classification and access to protein sequence
660 annotations. Nucleic Acids Res gky1100

661 28. Käll L, Krogh A, Sonnhammer ELL (2004) A Combined Transmembrane Topology and
662 Signal Peptide Prediction Method. J Mol Biol 338: 1027-1036.

663 29. Nielsen H (2017) Predicting Secretory Proteins with SignalP. In Kihara, D (ed): Protein
664 Function Prediction (Methods in Molecular Biology vol. 1611) pp. 59-73,
665 Springer.

666 30. Zhang Y-Z, Shen H-B (2017) Signal-3L 2.0: A hierarchical mixture model for enhancing
667 protein signal peptide prediction by incorporating residue-domain cross level
668 features. J Chem Inf Model 57: 988-999.

669 31. Steentoft C, Vakhrushev SY, Joshi HJ, Kong Y, Vester-Christensen MB, et al. (2013)
670 Precision mapping of the human O-GalNAc glycoproteome through SimpleCell
671 technology. EMBO J 32: 1478-1488.

bioRxiv preprint doi: https://doi.org/10.1101/607622; this version posted April 12, 2019. The copyright holder for this preprint (which was not certified by peer review) is the author/funder, who has granted bioRxiv a license to display the preprint in perpetuity. It is made available under aCC-BY 4.0 International license.

672 32. Gasteiger E, Hoogland C, Gattiker A, Duvaud S, Wilkins MR, et al. (2005) Protein
673 Identification and Analysis Tools on the ExPASy Server; (In) John M. Walker (ed):
674 The Proteomics Protocols Handbook, Humana Press. pp. 571-607.

675 33. Waterhouse A, Bertoni M, Bienert S, Studer G, Tauriello G, et al. (2018) SWISS-
676 MODEL: homology modelling of protein structures and complexes. Nucleic Acids
677 Res 46(W1): W296-W303.

678 34. Passerini A, Lippi M, Frasconi P (2011) MetalDetector v2.0: Predicting the Geometry
679 of Metal Binding Sites from Protein Sequence. Nucleic Acids Res 39: W288-
680 W292.

681 35. Sievers F, Wilm A, Dineen D, Gibson TJ, Karplus K, et al. (2011). Fast, scalable
682 generation of high-quality protein multiple sequence aligments using Clustal
683 Omega. Mol Syst Biol 7: 539.

684 36. Zuckerkandl E, Pauling L (1965) Evolucionary divergence and convergence in protein.
685 Edited in Evolving genes and proteins by V. Bryson and H.J. Vogel. Pp. 97-166.
686 Academic Press, New York.

687 37. Kumar S, Stecher G, Tamura K (2016) MEGA7: Molecular evolutionary genetic
688 analysis version 7.0 for bigger datasets. Mol Biol Evol 33: 1870-1874.

689 38. Buonanno F, Ortenzi C (2016) Cold-shock based method to induce the discharge of
690 extrusomes in ciliated protists and its efficiency. J Basic Microbiol 56: 586-590.

691 39. McArdle EW, Bergquist BL, Ehret CF (1980) Structural Changes in *Tetrahymena*
692 *rostrate* during Induced encystment. J Protozool 27: 388-397.

bioRxiv preprint doi: https://doi.org/10.1101/607622; this version posted April 12, 2019. The copyright holder for this preprint (which was not certified by peer review) is the author/funder, who has granted bioRxiv a license to display the preprint in perpetuity. It is made available under aCC-BY 4.0 International license.

693 40. Tiedtke A (1976) Capsule shedding in *Tetrahymena*. Naturwissenschaften 63: 93.

694 41. Hünseler P, Scheidgen-Kleyboldt G, Tiedtke A (1987)
695 Isolation and characterization of a mutant of *Tetrahymena thermophila* blocked
696 in secretion of lysosomal enzymes. J Cell Sci 88: 47-55.

697 42. Rawlinson NG, Gates MA (1989) A structural study of induced capsule formation in
698 the ciliate *Colpidium colpoda*. Trans Am Microsc Soc 108: 354-368.

699 43. Hausmann K (1978) Extrusive organelles in protists. Int Rev Cytol 52: 197-276.

700 44. Shih SJ, Nelson DL (1991) Multiple families of proteins in the secretory granules of
701 *Paramecium tetraurelia*: immunological characterization and
702 immunocytochemical localization of trichocyst proteins. J Cell Sci 100: 85-97.

703 45. Madeddu L, Gautier MC, Vayssié L, Houari A, Sperling L (1995) A large multigene
704 family codes for the polypeptides of the crystalline trichocyst matrix in
705 *Paramecium*. Mol Biol Cell 6: 649-659.

706 46. Adoutte A, Garreau de Loubresse N, Beisson J (1984) Proteolytic cleavage and
707 maturation of the crystalline secretion products of *Paramecium*. J Mol Biol 180:
708 1065-1080.

709 47. Gautier MC, Garreau de Lombresse N, Madeddu L (1994) Evidence for defects in
710 membrane traffic in *Paramecium* secretory mutants unable to produce
711 functional storage granules. J Cell Biol 124: 893-902.

bioRxiv preprint doi: https://doi.org/10.1101/607622; this version posted April 12, 2019. The copyright holder for this preprint (which was not certified by peer review) is the author/funder, who has granted bioRxiv a license to display the preprint in perpetuity. It is made available under aCC-BY 4.0 International license.

712 48. Tindall SH, De Vito LD, Nelson DL (1989) Biochemical characterization of the
713 *Paramecium* secretory granules. J Cell Sci 92: 441-447.

714 49. Glas-Albrecht R, Németh A, Plattner H (1990)
715 Secretory proteins and glycoproteins from *Paramecium* cells. Eur J Protistol 26:
716 149-159.

717 50. Maihle NJ, Satir BH (1986) Protein secretion in *Tetrahymena thermophila*.
718 Characterization of the major proteinaceous secretory proteins. J Biol Chem 261:
719 7566-7570.

720 51. Wolfe J (1988) Analysis of *Tetrahymena* mucocyst material with lectins and alcian
721 blue. J Protozool 35: 46-51.

722 52. Corfield AP, Berry M (2015) Glycan variation and evolution in the eukaryotes. Trends
723 Biochem Sci 40: 351-359.

724 53. Qin X, Jin P, Jiang T, Li M, Tan J, Wu H, Zheng L, Zhao J (2018) A human chondrocyte-
725 derived *in vitro* model of alcohol-induced and steroid-induced femoral
726 head necrosis. Med Sci Monit 24: 539-547.

727 54. Tas J (1977) The Alcian Blue and combined Alcian Blue-Safranin O staining of
728 glycosaminoglycans studied in a model system and in mast cell. Histochem J 9:
729 205-230.

730 55. Corfield AP (2015) Mucins: a biologically relevant glycan barrier in mucosal
731 protection. Biochim Biophys Acta 1850: 236-252.

bioRxiv preprint doi: https://doi.org/10.1101/607622; this version posted April 12, 2019. The copyright holder for this preprint (which was not certified by peer review) is the author/funder, who has granted bioRxiv a license to display the preprint in perpetuity. It is made available under aCC-BY 4.0 International license.

732 56. Gilligan DM, Satir BH (1983) Stimulation and inhibition of secretion in *Paramecium*:
733 role of divalent cations. J Cell Biol 97: 224-234.

734 57. Garofalo RS, Satir BH (1984) *Paramecium* secretory granule control: quantitative
735 studies on *in vitro* expansion and its regulation by calcium and pH. J Cell Biol 99:
736 2193-2199.

737 58. Satir BH. (1989) Signal transduction events associated with exocytosis in ciliates. J
738 Protozool 36: 382-389.

739 59. Kerboeuf D, Cohen J (1996) Inhibition of trichocyst exocytosis and calcium influx in
740 *Paramecium* by amiloride and divalent cations. Biol Cell 86: 39-43.

741 60. Satir B (1977) Dibucaine-induced synchronous mucocysts secretion in *Tetrahymena*.
742 Cell Biol Int Rep 1: 69-73.

743 61. Tiedtke A, Hünseler P, Rasmussen L. (1988) Growth requeriments of a new food-
744 vacuole-less mutant of *Tetrahymena*. Eur J Protistol 23: 350-353.

745
746
747
748
749
750
751
752
753
754
755

bioRxiv preprint doi: https://doi.org/10.1101/607622; this version posted April 12, 2019. The copyright holder for this preprint (which was not certified by peer review) is the author/funder, who has granted bioRxiv a license to display the preprint in perpetuity. It is made available under aCC-BY 4.0 International license.

FIGURE LEGENDS:

Figure 1.- Microphotographs obtained by differential interference contrast microscopy showing *P. dicentrarchi* trophonts after being incubated for 30 min with (A) preimmune serum, and (B) immune serum. The lower table shows the effect of different dilutions of turbot immune serum (antibody titre) and different incubation times on agglutination of ciliates (results expressed as percentages).

Figure 2.- Microphotographs obtained by differential interference contrast microscopy showing the sequence of changes after agglutination of the *P. dicentrarchi* trophonts caused by the addition of the turbot immune serum (up to 6 h incubation), including the presence of empty capsules (arrows).

Figure 3.-Microphotographs obtained by scanning electron microscope (SEM) of *P. dicentrarchi* trophonts, showing the changes in the ciliate surface after the addition of the turbot immune serum (up to 6 h incubation).

Figure 4.- (A,B) Microphotographs obtained by transmission electron microscopy (TEM) of *P. dicentrarchi* trophonts showing the structure of the two basic types of extrusomes: A) spherical extrusomes (circle) of mucocyst type (M), and a detailed enlargement of these structures in the upper right-hand side of the image; (B) fusiform extrusomes (circle) of trichocyst type (T), and a detailed enlargement of these structures in the upper right-hand side of the Image. C-D) amino acid sequence of *P. dicentrarchi* trichocyst matrix protein T2-A and T4-B (TMPT2A and TMPT4B, respectively). The shaded region indicates the prediction of a signal peptide between aa 1-18 (C) and aa 1-16 (D); bold red indicates the potential O-glycosylation sites of the proteins. Homology modelling (Swiss-model) including molecular weight prediction and theoretical isoelectric point (ip) of the TMPT2A (E) and TMPT4B (F) proteins of the *P. dicentrarchi* trichocyst matrix. Scale bar = 2 μm.

Figure 5.- A) CLUSTAL OMEGA (v.1.2.4) multiple sequence alignment of *P. dicentrarchi* trichocyst matrix protein T2-A from four representative ciliates of the phylum

bioRxiv preprint doi: https://doi.org/10.1101/607622; this version posted April 12, 2019. The copyright holder for this preprint (which was not certified by peer review) is the author/funder, who has granted bioRxiv a license to display the preprint in perpetuity. It is made available under aCC-BY 4.0 International license.

788 Ciliophora. B) Percent Identity Matrix - created by Clustal 2.1 C) Molecular Phylogenetic
789 analysis by Maximum Likelihood method. The tree is drawn to scale, with branch lengths
790 measured in the number of substitutions per site. The analysis involved 4 amino acid
791 sequences. All positions containing gaps and missing data were eliminated. The final
792 data set included a total of 367 positions. Evolutionary analysis was conducted with
793 MEGA7 software.
794
795 Figure 6.- A) CLUSTAL OMEGA (1.2.4) multiple sequence alignment of *P. dicentrarchi*
796 trichocyst matrix protein T4-B of four representative ciliates of the phylum Ciliophora B)
797 Percent Identity Matrix - created by Clustal 2.1 C) Molecular Phylogenetic analysis by
798 Maximum Likelihood method. The tree is drawn to scale, with branch lengths measured
799 in the number of substitutions per site. The analysis involved 4 amino acid sequences.
800 All positions containing gaps and missing data were eliminated. The data set included a
801 total of 354 positions. Evolutionary analysis was conducted with MEGA7 software.
802
803 Figure 7.- Histochemistry analysis of mucin production (a peptidoglycan component of
804 extrusomes) by safranin O staining of *P. dicentrarchi* trophonts after incubation with A)
805 control serum, B) immune turbot serum for 30 min, C) immune turbot serum for 2 h, D)
806 with immune turbot serum for 6h.
807
808 Figure 8.- (A) SDS-PAGE analysis of the recombinant *P. dicentrarchi* trichocyst matrix
809 protein T2-A (rTMPT2A), lane 1. MW: Molecular weight markers in kD. (B) FELISA of
810 levels of TMPT2A expressed by the trophonts incubated for 30 min and 6 h with the
811 turbot immune serum. Values are means ± standard errors. The symbol indicates a
812 significant difference ($P < 0.01$) relative to the control (time 0). (C) Microphotographs
813 obtained by confocal / phase contrast microscopy of *P. dicentrarchi* trophonts incubated
814 with immune serum for different times. The images correspond to the combination of a
815 visible image and an immunofluorescence (green signal) using a recombinant mouse
816 antibody anti-*P. dicentrarchi* TMPT2A and revealed with an anti-mouse rabbit antibody
817 conjugated with FITC.
818

bioRxiv preprint doi: https://doi.org/10.1101/607622; this version posted April 12, 2019. The copyright holder for this preprint (which was not certified by peer review) is the author/funder, who has granted bioRxiv a license to display the preprint in perpetuity. It is made available under aCC-BY 4.0 International license.

819 Figure 9.- (A) Levels of mRNA expression of the genes that encode the *P. dicentrarchi*
820 trichocyst matrix protein T2-A (TMPT2A) and *P. dicentrarchi* trichocyst matrix protein
821 T4-B (TMPT4B) in ciliates incubated for different lengths of time with turbot immune
822 serum and dibucaine (D). The results are expressed as the relative gene expression
823 versus the *P. dicentrarchi* elongation factor 1-alpha (EF1α). (B) Calcium response of
824 trophonts stimulated with turbot immune serum (ITS) and Hanks' balanced salt solution
825 (HBSS without Ca^{2+}, Mg^{2+}, and phenol red) quantified using the Fluo-4 NW calcium assay
826 kit. The time course of the increase in fluorescence by min (ΔF/min) of cell-permeable
827 fluorescent dye reflects the rates of dye-loading of cells by passive uptake of the AM
828 esters and the influx of calcium through membrane channels or release from
829 intercellular stores. The values at each data point are the mean $\pm$ standard error (SE) for
830 five replicates. Asterisks indicate a statistically significant difference (P<0.01) relative to
831 control (time 0).

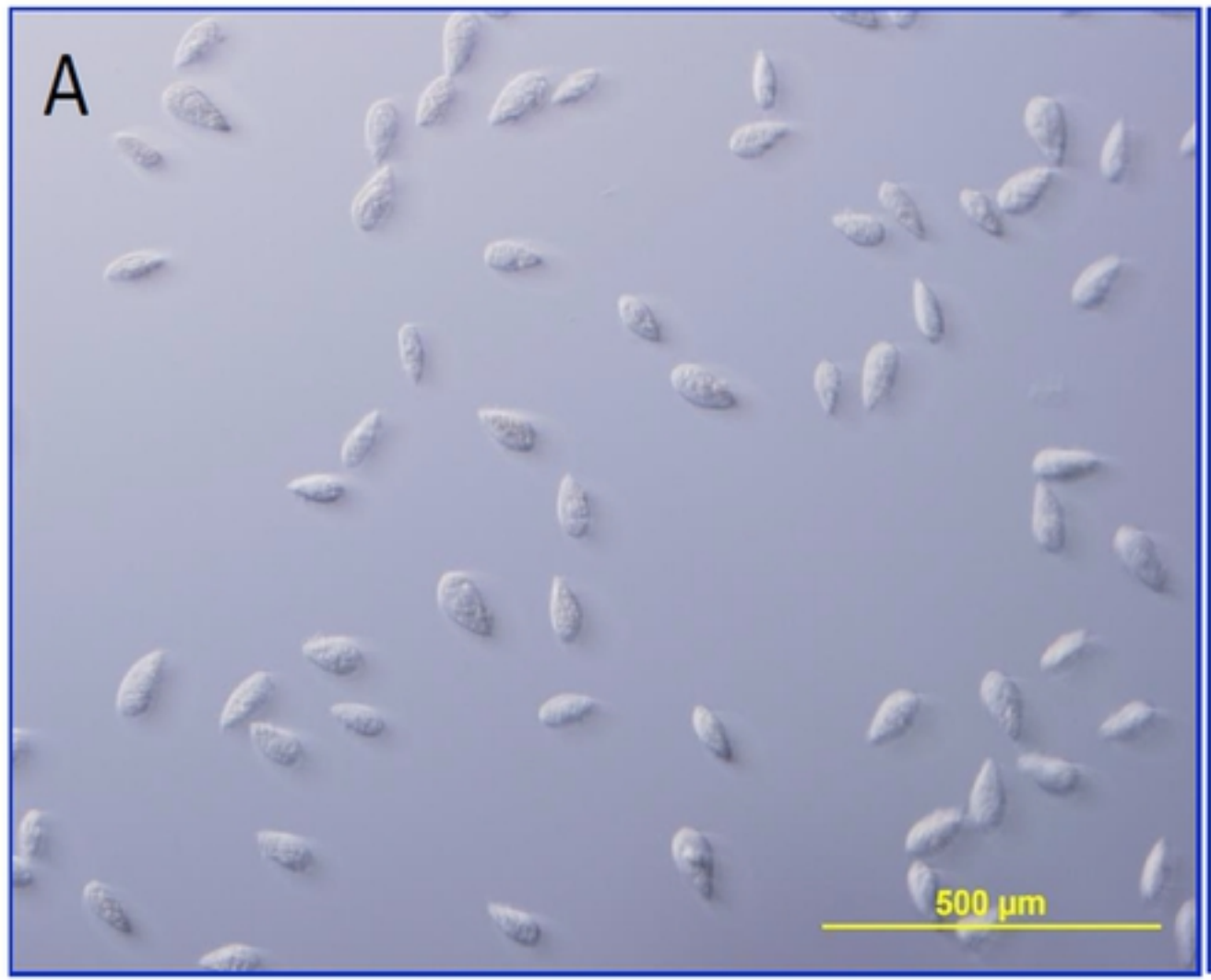

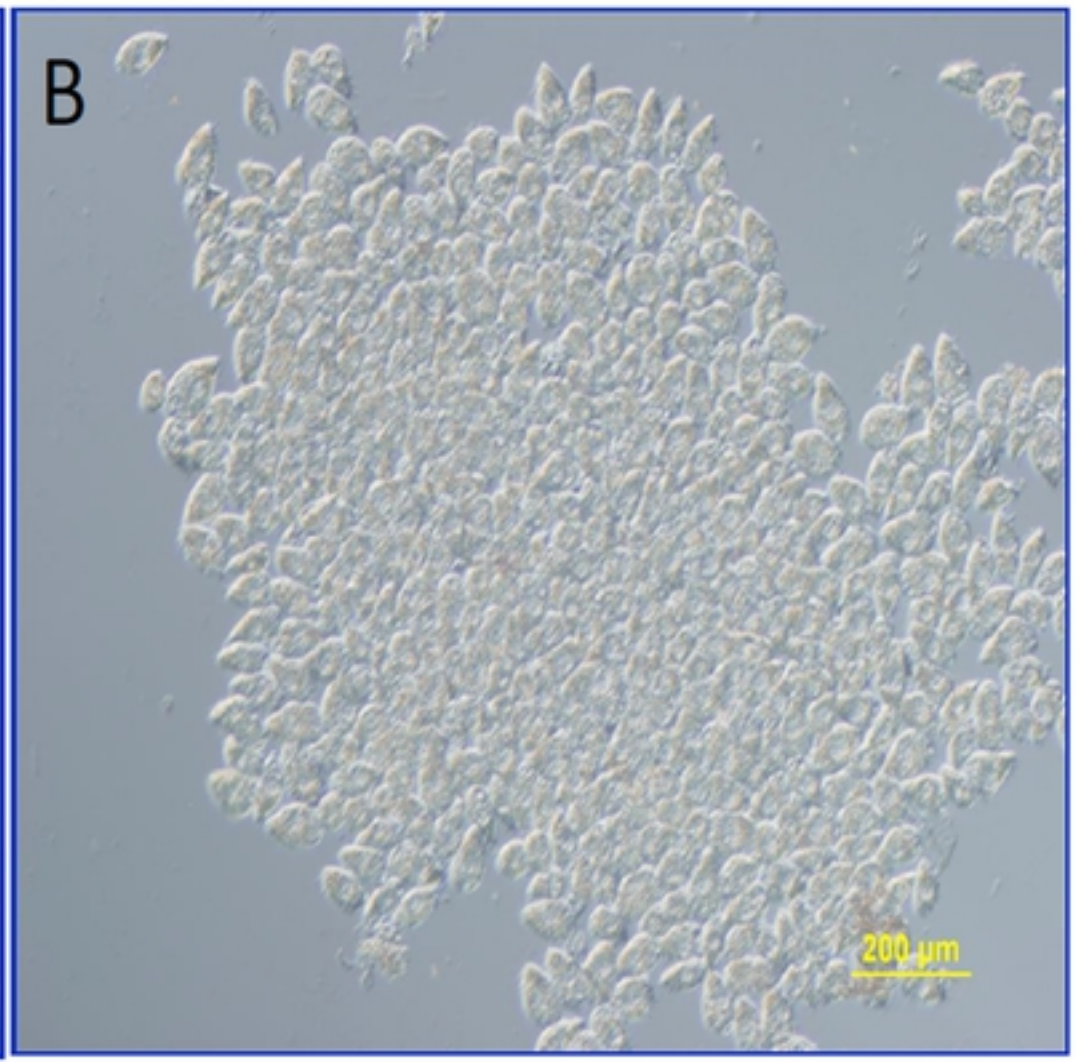

Serum titre								
1:25			1:50			1:100		
15 min	30 min	60 min	15 min	30 min	60 min	15 min	30 min	60 min
27%	59%	77%	26%	59%	85%	31%	38%	46%

Figure 1

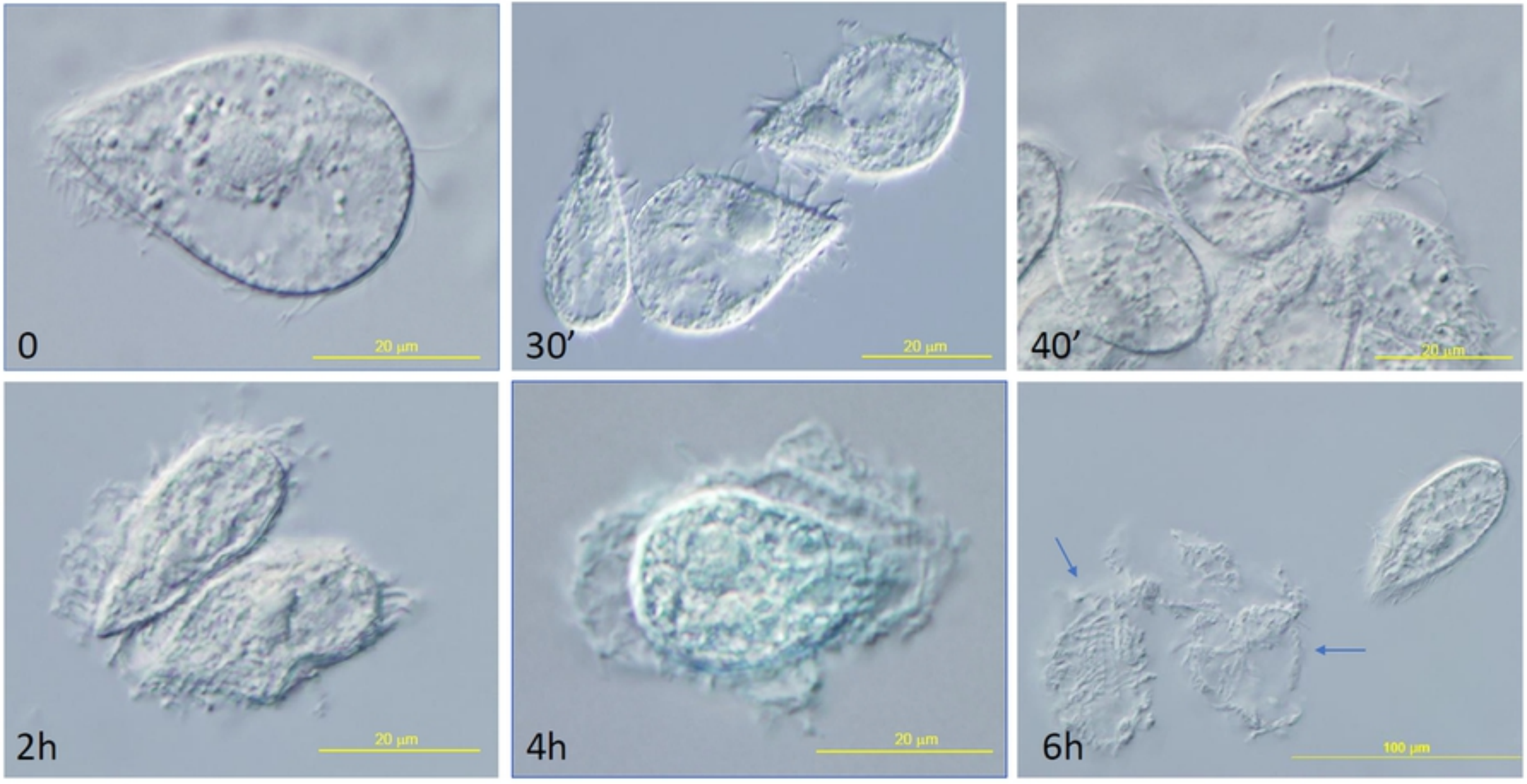

Figure 2

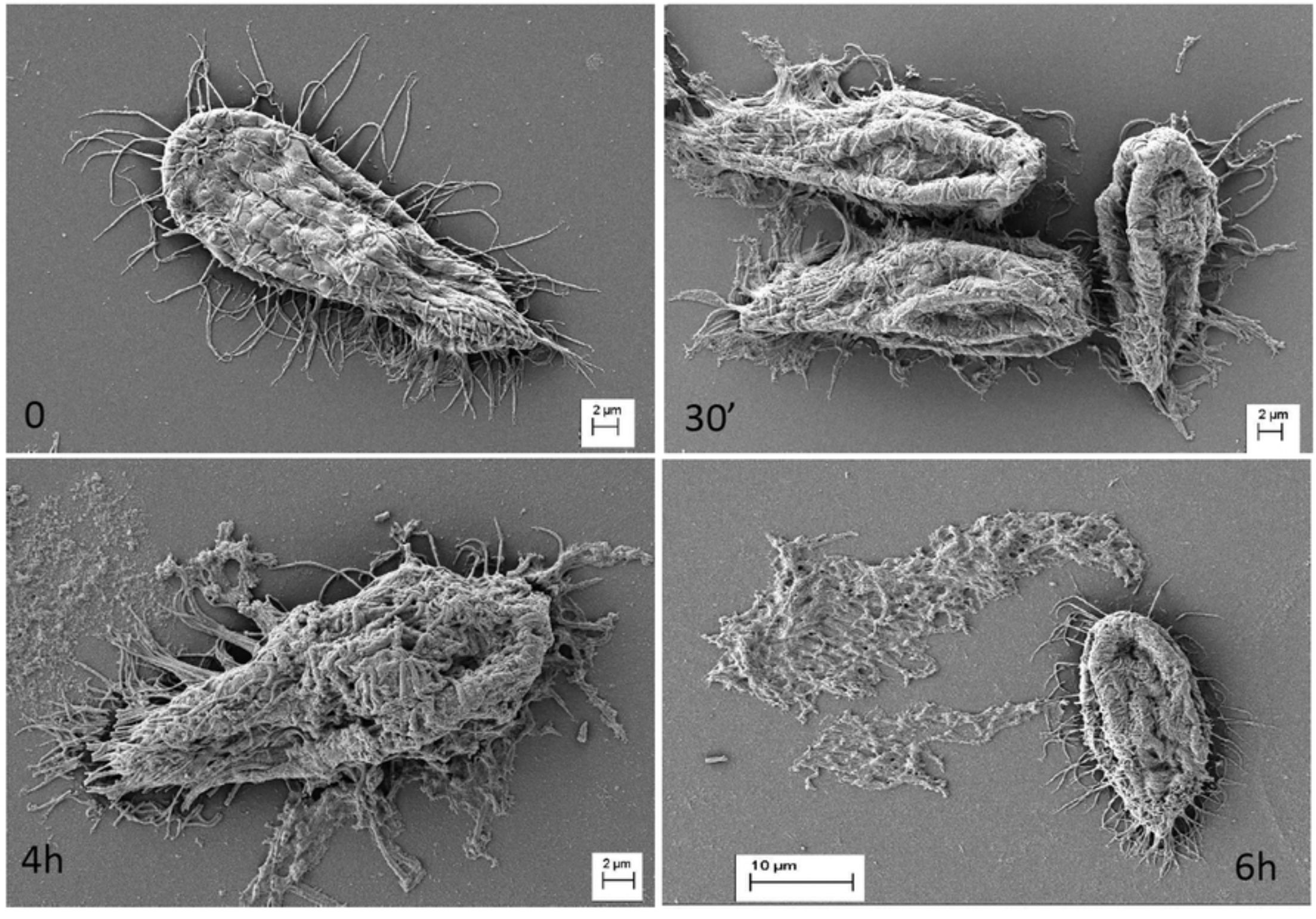

Figure 3

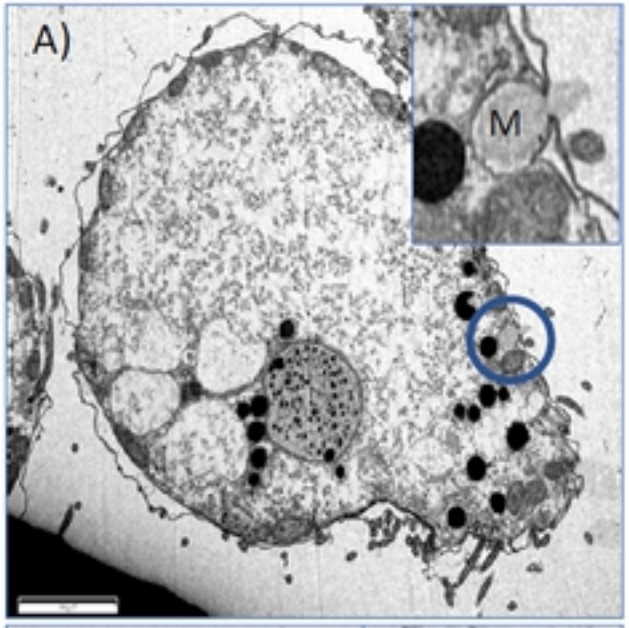

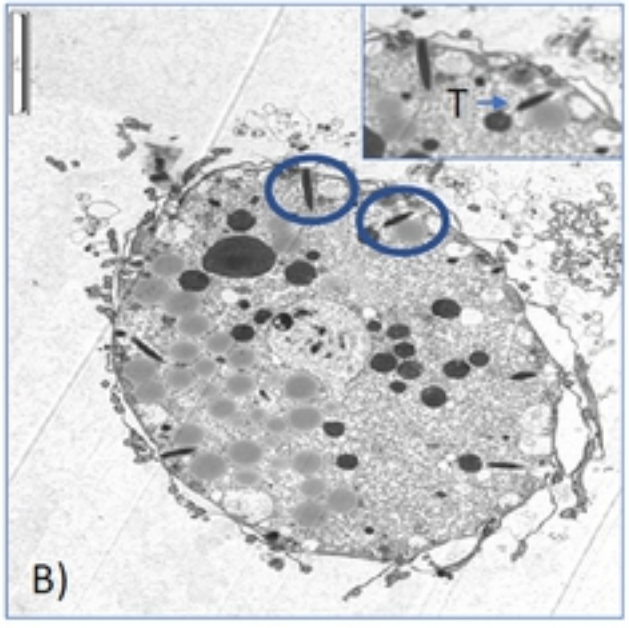

C) MRVLTALFACVLVLGAFAVTDPEIASVVRKMENSKYGKTLLDTIALQMEA
GDPVQDLIDMLQETEDGLERAQDEDDEFIRNEQERCDVDLARLQGEIED
AARRIAELQAELDEKIPIRDEKVRVLGEKNEWKDHLEAKVAEIDSQKVLKD
QEWAEEQEQHDQAQYVIEKAKTIIVEALKANSFLQKGNTAFAQVSSHF
AKHSKTHFKRQSWSKIFNLLSQITSSAPVQADQGSVQKVIDLCDSLLD
KISESREIERRDYQHWMEEYKNFRNQLLDKLVQVNKEIADLEQQIAALNK
RIAQCQAEKADQEERFRQKTSEHEDLLQYCDDANVAYAKRRESRNDERE
VVSDAIGLLQSKLRTFRQYVSERMGSDVKRAD

D) MKRVAIILLLTVLSQCGIQRSPARLSDTKTVLAEMDKDSFGSTILSAVAL
NAATGNPVEEITVLIEEIVEQLTTEQNQADGLNTQNEASCETNIDNLN
QQIAQTKATIESTENALKINSEILKDAKVTLAQANRDFDEVVESIDQG
SQQRRADHERWVEEDYANAISIATLEEGVKLINHMIHGVEFTQIKSRY
EKVLDKLKEDNNKHASLFKPLISSLTQLATRLNYENVMKILELLNNIRLTI
AEEQQQAKEAENIASEDWQKLLNHLAAEKQRLGDKKARLSSLIEATT
TLLEQYRQSLENNKVQLENYSQTLVNETQRCSQQAETYAVESAERAR
ELEILERLLEHMREKYNQVSEYVSSRVYSDF

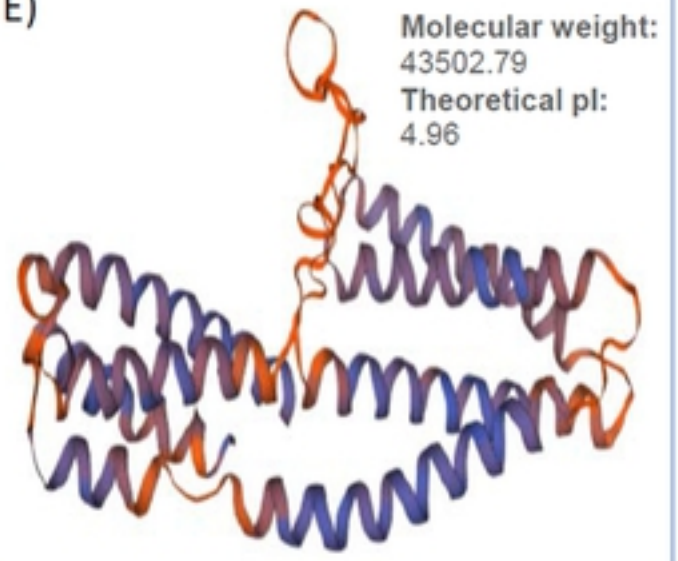

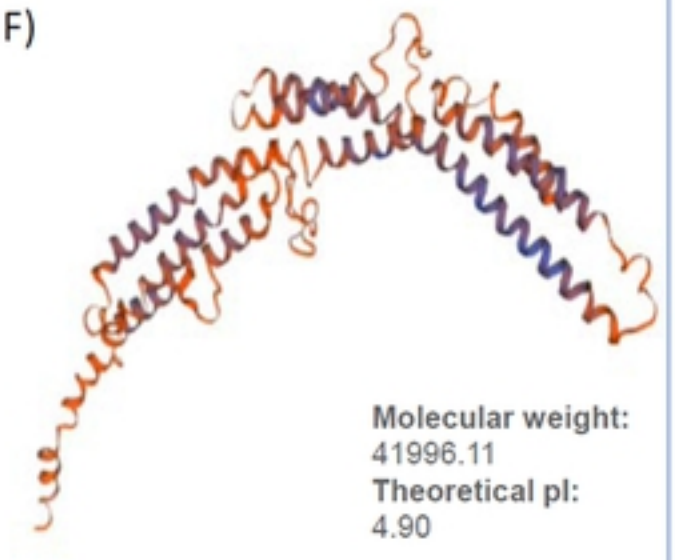

Figure 4

A)

B)

	Paramecium	*Ichthyophthirius*	*Philasterides*	*Tetrahymena*
Paramecium	100.00	30.91	26.90	24.60
Philasterides		100.00	32.97	30.29
Ichthyophthirius			100.00	37.03
Tetrahymena				100.00

C)

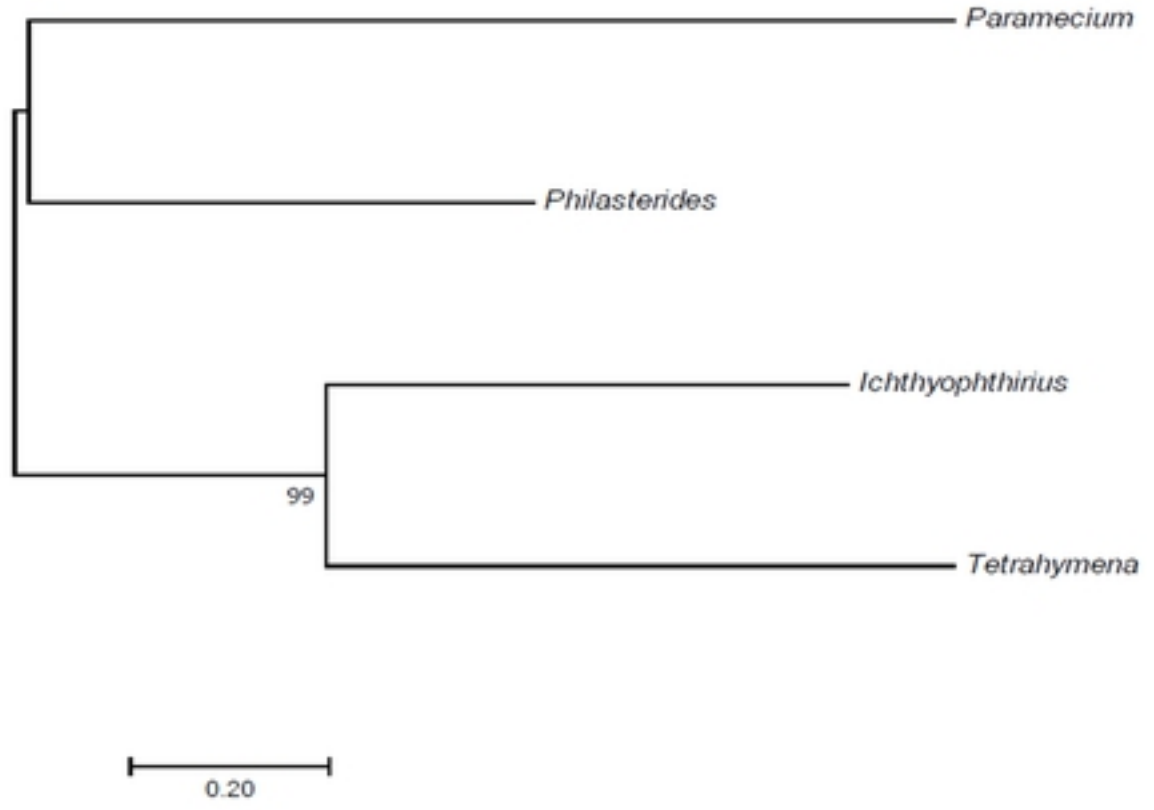

Figure 5

A)

B)

	Paramecium	*Ichthyophthirius*	*Philasterides*	*Tetrahymena*
Paramecium	100.00	28.65	31.68	30.23
Ichthyophthirius		100.00	36.11	36.97
Philasterides			100.00	40.06
Tetrahymena				100.00

C)

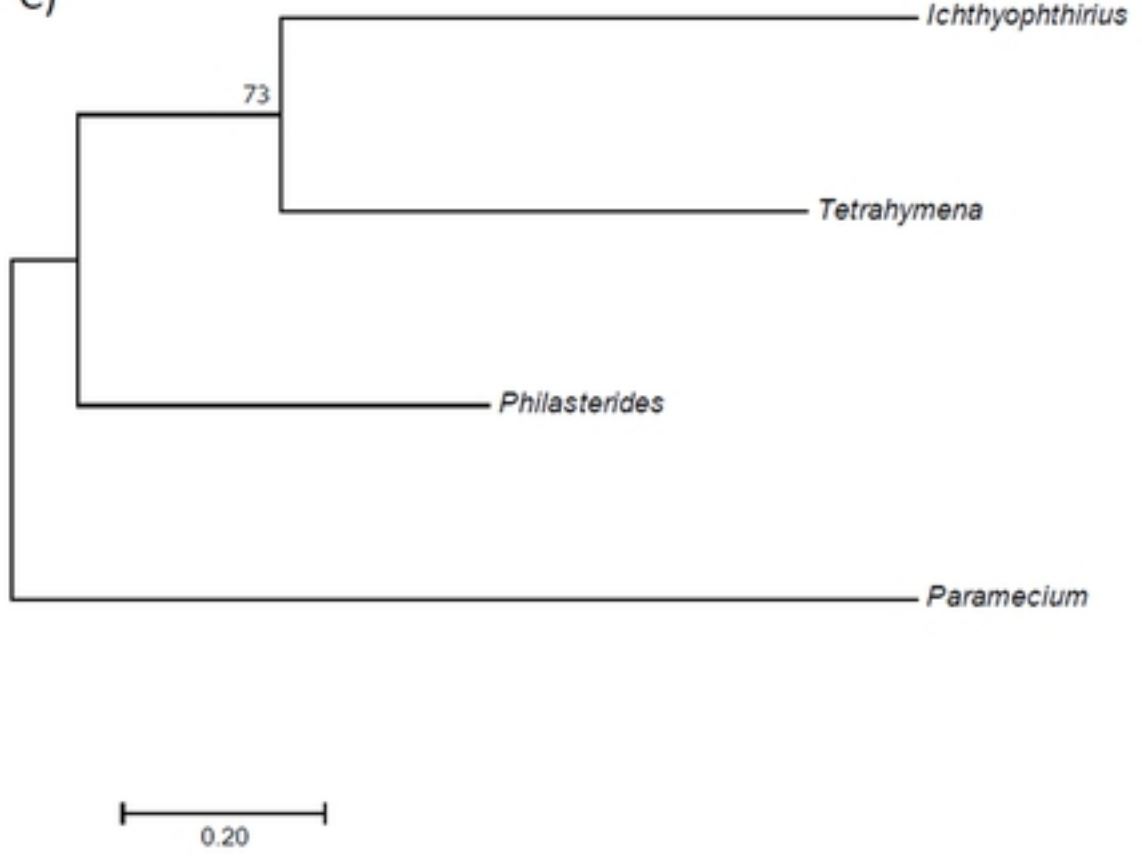

Figure 6

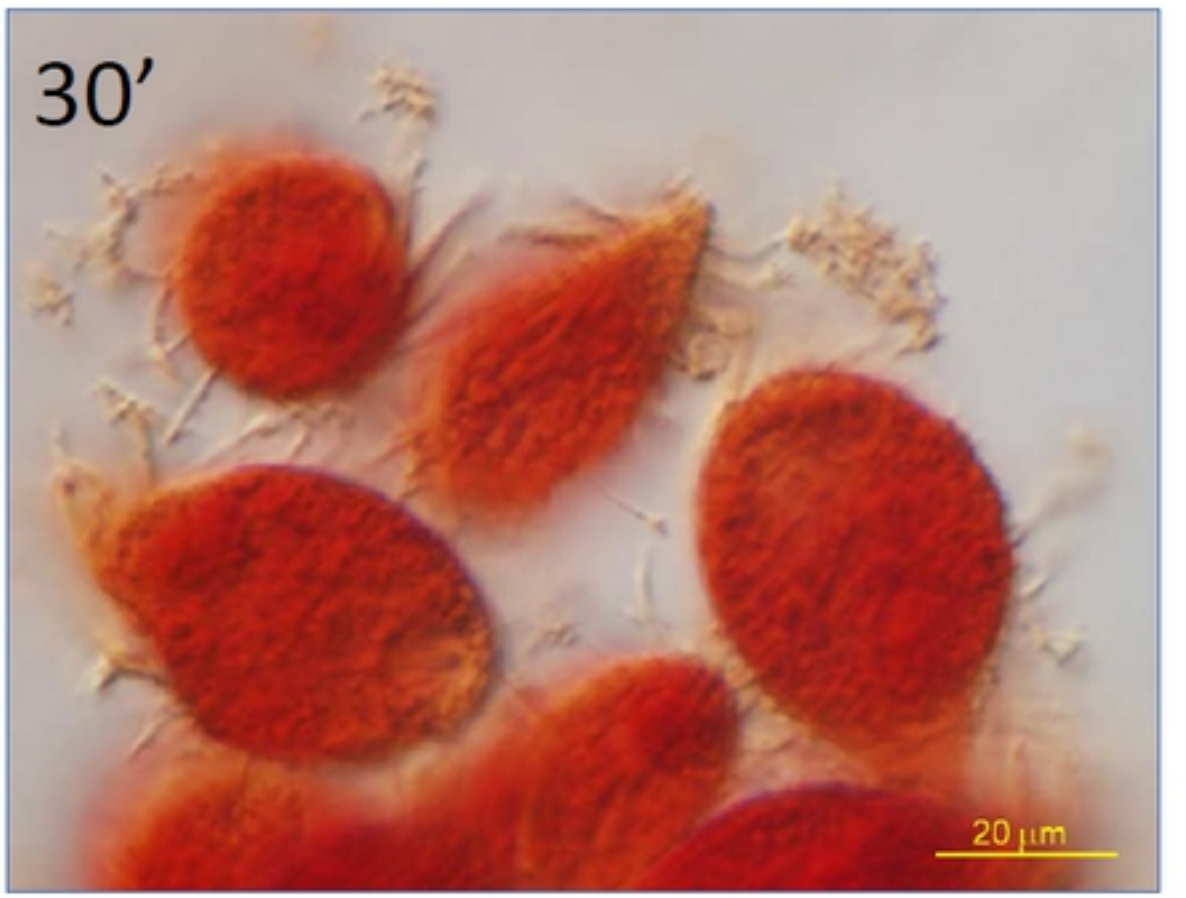

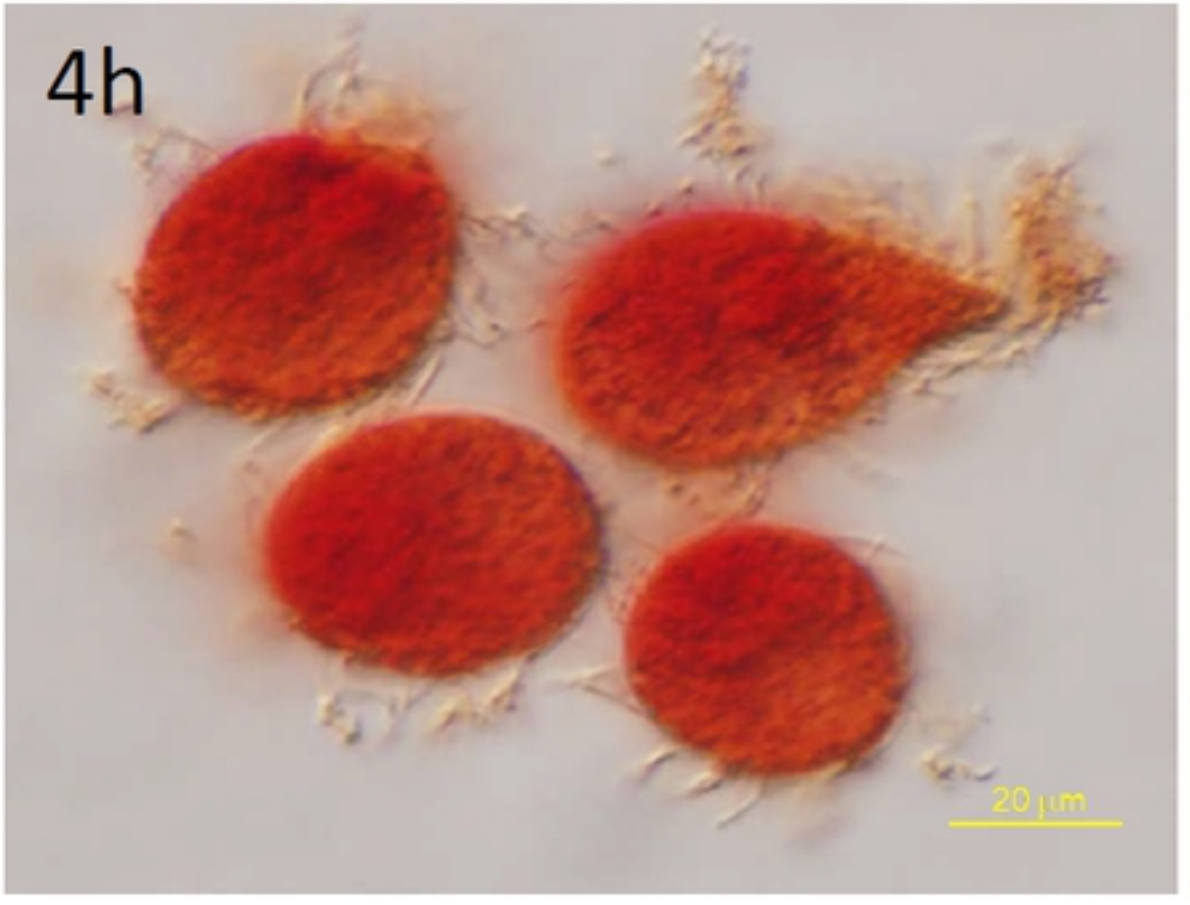

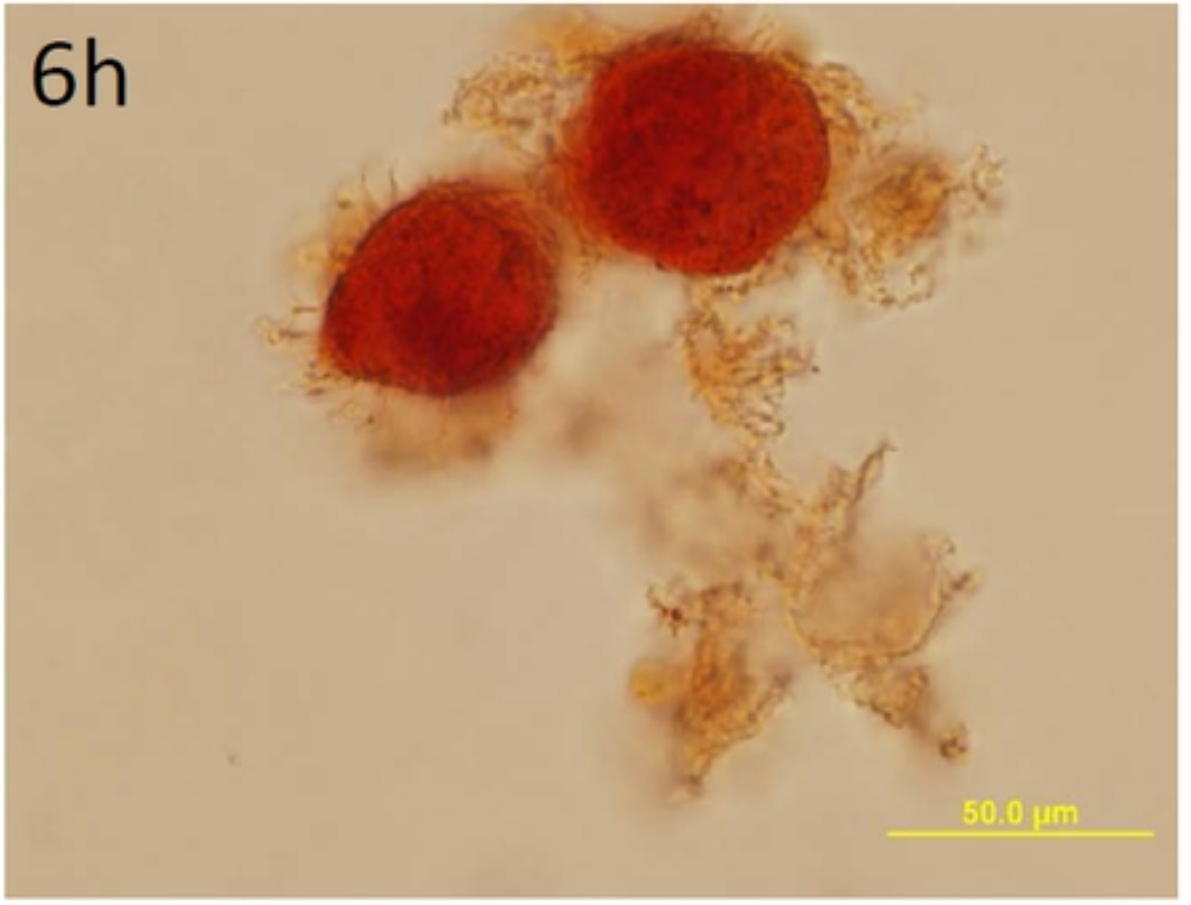

Figure 7

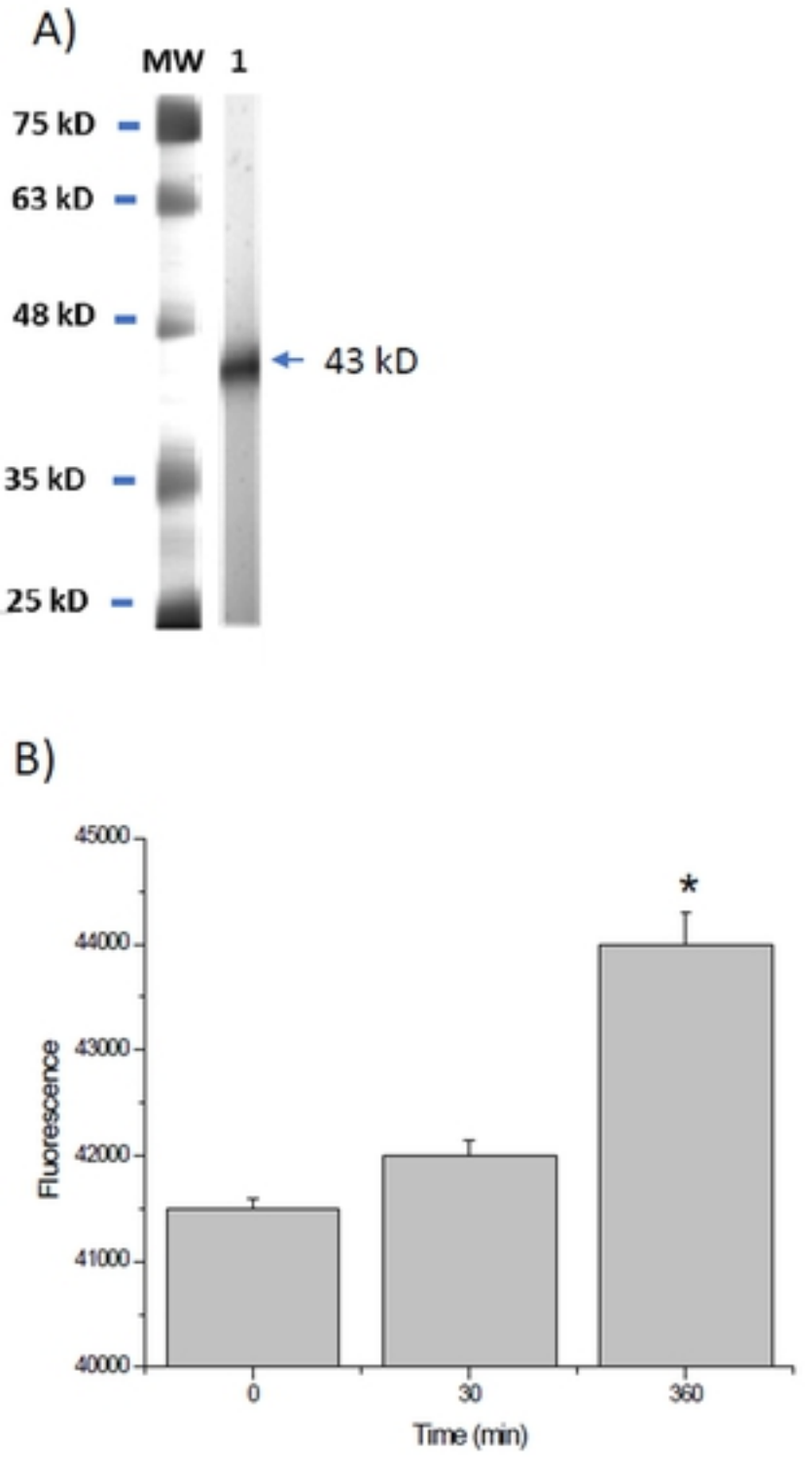
A)
MW
1
75 kD
63 kD
48 kD
43 kD
35 kD
25 kD
B)
Fluorescence
45000
44000
43000
42000
41000
40000
*
0
30
360
Time (min)
C)
0
30'
4h
6h
20 µm
20 µm
20 µm
20 µm

Figure 8

Figure 9